THE JOURNAL OF BIOLOGICAL CHEMISTRY VOL. 292, NO. 7, pp. 2571–2585, February 17, 2017

Tribbles Pseudokinase 3 Induces Both Apoptosis and Autophagy in Amyloid-β-induced Neuronal Death*

Received for publication, June 22, 2016, and in revised form, December 22, 2016 Published, JBC Papers in Press, December 23, 2016, DOI 10.1074/jbc.M116.744730

Suraiya Saleem and Subhas Chandra Biswas[1]

From the Cell Biology and Physiology Division, Council of Scientific and Industrial Research-Indian Institute of Chemical Biology, 4 Raja S. C. Mullick Road, Kolkata 700032, India

Edited by Paul E. Fraser

Amyloid-β (Aβ)-induced neuron death is considered central to the pathogenesis of Alzheimer's disease (AD). Among several death modalities, autophagy and apoptosis play important roles in Aβ-induced neuron death suggesting that there may be regulatory mechanisms that initiate both cell death pathways. However, molecules that govern both pathways have not been identified. Here, we report that, upon Aβ treatment, tribbles pseudokinase 3 (Trib3, an ortholog of *Drosophila Tribbles*) is up-regulated in neurons both *in vivo* and *in vitro*. Increased Trib3 levels inhibited the activity of the kinase Akt by interacting with it. As a result, forkhead box O1 (FoxO1), a transcription factor that is negatively regulated by Akt, was activated, translocated to the nucleus, and induced the pro-apoptotic gene *BCL2-like 11* (Bim). Conversely, FoxO1 responded to Aβ insult by binding to the *Trib3* gene promoter, enhancing its expression. Our investigations further revealed that Trib3 also induces autophagy. We found that Trib3 indirectly activates unc-51-like autophagy-activating kinase1 (Ulk1) by impeding phosphorylation of, and thus inactivating, a negative regulator of Ulk1, mechanistic target of rapamycin. Ulk1 activation augmented autophagosome formation and reduced autophagy flux. Thus, Trib3 was required for formation of autophagosomes, which accumulated in neurons as autophagic flux was thwarted. Most importantly, silencing endogenous Trib3 strongly protected neurons from Aβ insult. Our results suggest that a self-amplifying feed-forward loop among Trib3, Akt, and FoxO1 in Aβ-treated neurons induces both apoptosis and autophagy, culminating in neuron death. Thus, Trib3 may serve as a potential therapeutic target for AD.

Alzheimer's disease (AD)[2] is a progressive neurodegenerative disorder that is emerging as the leading cause of dementia today. It involves a gradual deterioration in several cognitive domains, including loss of memory. The two pathognomonic features of the disease include plaques of β-amyloid (Aβ) and neurofibrillary tangles of hyperphosphorylated Tau (1, 2). The disease is also characterized by accumulation of misfolded proteins, compromised autophagy, enhanced oxidative stress, and metabolic perturbations (3–5). Disturbances in cellular homeostasis lead to increased endoplasmic reticulum (ER) sensitivity, which is a characteristic feature in AD. Excessive ER stress is detrimental to neurons because it can switch on an apoptotic program and also can trigger inflammatory responses (6). In contrast, inappropriate aggregation of waste proteins and shoddy organelles induce autophagy via ER stress (7). Mounting evidence reveals the presence of accumulated autophagosomes and defective autophagy flux in the pathogenesis of AD (8, 9). It has also been demonstrated that Aβ accumulates in autophagic vacuoles, and inappropriate clearance of these vacuoles, impaired autophagic-lysosomal degradation, promotes the extracellular deposition of it thus exacerbating the pathological condition in AD (10–13).

Recent studies indicate the dynamic participation of ER stress in activating autophagy and promoting apoptosis of tumor cells, wherein Trib3 (Tribbles homolog 3) leads the saga by inhibiting Akt and mTORC1 in turn leading to enhanced autophagy and subsequent apoptosis in hepatocarcinoma cells and glioma cells (14, 15). Trib3 is a mammalian ortholog of the *Drosophila Tribbles* gene and is also known as neuronal death-inducible putative kinase/Sink1/Skip3 (16). Trib3 is responsible for a plethora of functions ranging from glucose regulation, migration of tumor cells, suppressing differentiation of adipocytes, and cell cycle control (17–20). It was identified as a novel ER stress-inducible gene that, when up-regulated, activated several genes involved in cell death during ER stress (21). Trib3 is also shown to be elevated by several stresses, including hypoxia, 6-hydroxydopamine, growth factor deprivation, anoxia, and ethanol exposure (16, 22–28). It has also been shown that Trib3 is elevated in Parkinson's disease brains and mediates neuron death in various Parkinson's disease models (27). Trib3 is a pseudokinase because it lacks the catalytic residues required for its kinase function (29, 30). Bioinformatic analysis of Trib3 protein reveals the presence of a number of conserved domains that account for its ability to interact with numerous protein-binding partners (25, 31–33).

AD has well been characterized as a multifactorial disease where a single unwavering approach to tackle the disease might

* This work was supported by one of the 12th Five Year Plan Projects, miND BSC0115, from the Council of Scientific and Industrial Research, Government of India. The authors declare that they have no conflicts of interest with the contents of this article.

[1] To whom correspondence should be addressed: Cell Biology and Physiology Division, Council of Scientific and Industrial Research-Indian Institute of Chemical Biology, 4 Raja S. C. Mullick Rd., Kolkata 700032, India. Tel.: 91-33-24995941; Fax: 91-33-24735197; E-mail: biswassc@gmail.com or subhasbiswas@iicb.res.in.

[2] The abbreviations used are: AD, Alzheimer's disease; FoxO, Forkhead box, class O; Aβ, β-amyloid; PC12, pheochromocytoma cells; Bim, Bcl-2 interacting mediator of cell death; mTOR, mammalian target of rapamycin; LC3, light chain 3; ER, endoplasmic reticulum; DIV, days *in vitro*; HFIP, 1,1,1,3,3,3-hexafluoro-2-propanol.

be ineffective. A combination of treatment strategies may prove beneficial in this arena. Several approaches have been studied, yet most of them have met with failure at the stage of clinical trials. Because the Aβ cascade hypothesis holds the spotlight of the pathogenesis of the disease, targeting Aβ proves to be a promising approach (34, 35). Apart from this, a complementary therapy is imperative to impede the toxicity due to Aβ, the complete removal of which is difficult. Hence, a complete understanding of the molecular mechanism of Aβ-induced death is quintessential. In this study, we have investigated the role of Trib3 in neuronal death induced by Aβ. It appears that Trib3 is induced and promotes death of neurons by both apoptosis and autophagy in response to Aβ.

Results

Aβ Treatment Induces Trib3 mRNA and Protein Levels in Vitro and in Vivo—Accumulating evidence implicates Aβ oligomers as the principal cause of AD pathogenesis (36, 37). Oligomeric Aβ at a concentration of 1.5 μM leads to significant death of primary cortical and hippocampal neurons after 24 h of exposure (38). We determined the levels of Trib3 in neurons after Aβ exposure. We found that Trib3 levels were increased in cultured cortical neurons following Aβ(1–42) treatment. To check the specificity of the action of Aβ(1–42), we used a reverse peptide, Aβ(42–1), and we found that the reverse peptide Aβ(42–1) has no effect on Trib3 levels in the primary cortical neurons (data not shown). Trib3 transcript levels were significantly increased as early as after 4 h and about 3-fold increased after 8 h of Aβ(1–42) treatment as detected by semi-quantitative (Fig. 1*A*) and real time PCR (Fig. 1*B*). Protein levels of Trib3 were also significantly increased within 4 h and they were about 3- and 3.5-fold increased after 8 and 16 h of Aβ treatment, respectively (Fig. 1, *C* and *D*). Thus, Trib3 expression was elevated well before cell death became apparent (see below and Fig. 2*C*).

Next, we investigated whether this increase of *Trib3 in vitro* is also reflected in *in vivo* conditions. Reports reveal that oligomeric Aβ when infused into adult rat brains results in Aβ deposition, caspase-3 activation, and neuronal cell loss in the vicinity of Aβ infusion (38). In our study adult rats were infused with Aβ or PBS on the right hemisphere of their brains. 21 days later these animals were sacrificed, and their brains were fixed, cryosectioned, and then immunostained with Aβ(1–42) antibody to check Aβ deposition in the site of Aβ infusion (Fig. 1*E*). Adjacent sections were also co-immunostained with Trib3 and NeuN (a neuronal marker) antibodies. Nuclei were stained with Hoechst dye. Results revealed marked up-regulation of Trib3 in Aβ-infused rat brains as compared with PBS-infused rat brains (Fig. 1, *F* and *G*). Because synthetic Aβ may behave differently from naturally secreted Aβ, brain sections of APPswe-PS1de9 (Swedish mutation in amyloid precursor protein and PS1 mutation) transgenic mice, which naturally secrete Aβ, were also examined for Trib3 expression. The presence of Aβ plaques in the transgenic mouse brain was checked by Congo red staining (Fig. 1*H*). Transgenic and control littermate mouse brains were cryosectioned and co-immunostained with Trib3 and NeuN antibodies. Hoechst dye was used to stain the nuclei. It was observed that there was a significant increase in Trib3 levels in transgenic mice as compared with the control littermates (Fig. 1, *I* and *J*). Therefore, our study indicates that Trib3 expression is increased in neurons upon exposure to Aβ *in vitro* and *in vivo*. To find the role of Trib3 in Aβ-induced neuronal cell death *in vivo*, we performed immunostaining of Trib3 along with TUNEL assay in sections in the vicinity of Aβ infusion. We observed that increased Trib3 expression co-localized with TUNEL-positive cells in Aβ-infused rat brain sections as compared with PBS-infused rats (Fig. 1*K*, see *arrows*). This indicates the role of Trib3 in Aβ-induced neuronal cell death *in vivo*.

Trib3 Plays an Essential Role in Neuronal Death Evoked by Aβ—We next assessed whether Trib3 is necessary in evoking neuronal death in response to Aβ. We interfered with the expression of Trib3 using previously described shRNA constructs (23). The Trib3 shRNA construct efficiently blocked induction of Trib3 by Aβ in neuronally differentiated (primed) PC12 cells (Fig. 2, *A* and *B*). Primary cultured cortical neurons were then transfected with this shRNA construct (shTrib3) or a control shRNA construct (shRand) and maintained for 48 h followed by oligomeric Aβ treatment (1.5 μM). Transfected live green cells were monitored and counted under a fluorescence microscope at different time intervals. Down-regulation of Trib3 by shRNA blocked neurodegeneration as evident from the retention of neuronal processes and caused significant survival of these neurons compared with shRand-transfected neurons even after 72 h of Aβ treatment (Fig. 2, *C* and *D*).

A similar experiment with cultured hippocampal neurons revealed that down-regulation of Trib3 also provided significant protection of hippocampal neurons from Aβ-induced neurotoxicity (Fig. 2, *E* and *F*). Hippocampal neurons expressing shTrib3 not only showed increased viability as compared with shRand-transfected neurons but also displayed enhanced retention of neurites and overall neuronal morphology (Fig. 2, *E* and *F*). Furthermore, we quantitatively assessed the retention of neurites and neuronal networks in shTrib3-transfected hippocampal neurons after Aβ treatment by Sholl analysis as described (38, 39). Single hippocampal neurons transfected with either shTrib3 or shRand were analyzed by ImageJ (National Institutes of Health) as described under "Experimental Procedures." Results revealed that the number of crossings remained almost same before and after treatment of Aβ in the case of shTrib3-transfected neurons, although there was a drastic reduction in the number of crossings in shRand-transfected neurons (Fig. 2*G*). Furthermore, we found that down-regulating Trib3 retains mitochondrial membrane potential (Fig. 2*H*), maintains post-synaptic membrane integrity (Fig. 2*I*), and decreases nuclear localization of cleaved caspase3 (Fig. 2*J*) even in Aβ-treated conditions. We also found a similar protective effect of shTrib3 on neuronal PC12 cells upon Aβ treatment (data not shown). Taken together, these results suggest that Trib3 plays a necessary role in mediating neuron degeneration and death evoked by Aβ toxicity.

Trib3 Negatively Regulates Akt upon Aβ Treatment—It has been shown that Trib3 blocks Akt activity by physically interacting with it in various non-neuronal cells (40–42). As phospho-Akt level is reported to be markedly reduced in AD brain (43), we tested whether Trib3 also negatively regulates Akt in neuronal cells in response to Aβ. Primary cultures of cortical

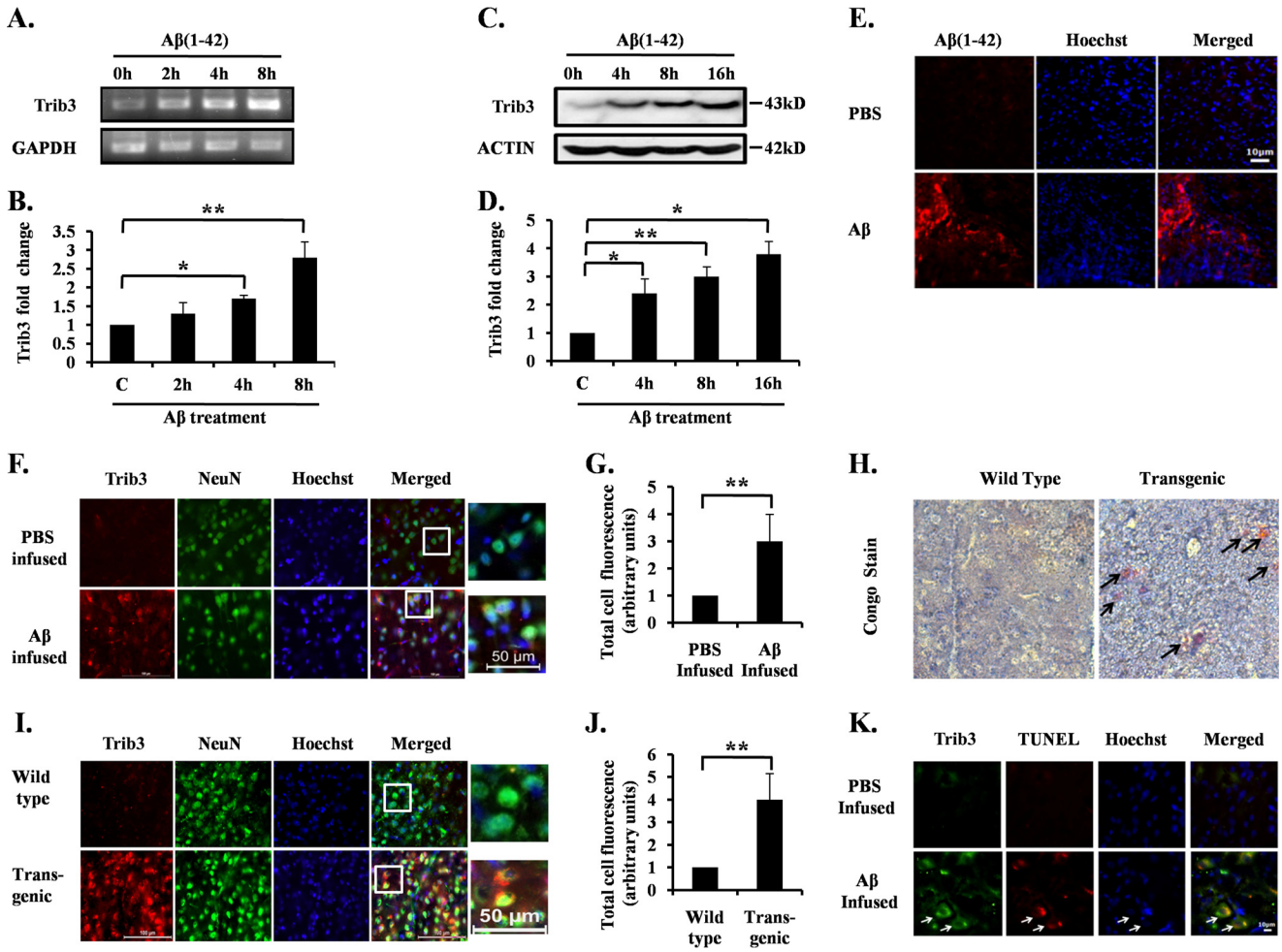

FIGURE 1. ***Trib3* mRNA and protein levels are elevated in response to Aβ *in vitro* and *in vivo*.** Primary rat cortical neurons (7DIV) were treated with oligomeric Aβ 1.5 μM for the indicated times. *A,* total RNA was isolated, subjected to reverse transcription, and analyzed by semi-quantitative PCR using Trib3 primers. GAPDH was used as loading control. *B,* graphical representation of fold changes in Trib3 transcript level upon Aβ treatment to rat cortical neurons for the indicated times by quantitative real time PCR. GAPDH was used as loading control. Data represent mean ± S.E. of three independent experiments. *, $p < 0.05$; **, $p < 0.01$. *C,* primary cultured rat cortical neurons were treated with Aβ for the times indicated. Total cell lysates were subjected to Western blotting analysis for Trib3 levels. A representative immunoblot of three independent experiments with similar results is shown. Actin was used as loading control. *D,* graphical representation of the Trib3 protein levels as quantified by densitometry of Western blottings in cortical neurons subjected to Aβ treatment for different time points. Data are expressed relative to untreated control. Data represents mean ± S.E. of three independent experiments. *, $p < 0.05$; **, $p < 0.01$. *E,* brain sections of the infused rats were immunostained with Aβ(1–42) antibody to check the presence of Aβ plaques in the infused brain area. *Upper panel* shows immunostaining of Aβ(1–42) antibody from brain sections of rats infused with PBS. *Lower panel* shows brain section immunostained with Aβ(1–42) antibody of Aβ-infused rat brains. *F,* adult rat brains were infused with either Aβ or PBS in the right hemispheres. 21 days later, the animals were sacrificed; brains were then cryosectioned, and sections were co-immunostained with antibodies for Trib3 and NeuN. Hoechst dye was used to stain nuclei. A representative image of one of the brain sections with similar results in each case is shown here. Images were taken using an inverted fluorescence microscope. *G,* graphical representation of corrected total cell fluorescence of Trib3 in PBS-infused and Aβ-infused brain sections. Difference in the intensity of Trib3 staining is quantified by ImageJ as described under "Experimental Procedures." Data represent mean ± S.E. of 30 different cells from three independent experiments. **, $p < 0.001$. *H,* Congo red staining of brain slices from transgenic and wild-type mice. Transgenic mouse brain shows the presence of amyloid plaques (shown by *arrow*), whereas such plaques were absent in the wild-type brain tissue. Representative images of six sections from three animals of each group with similar results are shown here. Images were taken under ×5 objective. *I,* level of Trib3 expression was analyzed in brain sections obtained from AβPPswe-PS1de9 transgenic mice and control littermates. Brain sections from transgenic and control mice were co-immunostained with Trib3 and NeuN antibodies. Nuclei were stained with Hoechst. Representative image of one of the brain sections with similar results in each case is shown here. *J,* graphical representation of corrected total cell fluorescence of Trib3 in transgenic and wild-type brain sections. Difference in intensity of Trib3 staining is quantified by ImageJ as described under "Experimental Procedures." Data represent mean ± S.E. of 30 different cells from three independent experiments. **, $p < 0.001$. *K,* brain sections from Aβ and PBS infused rats were analyzed for TUNEL assay and then immunostained for Trib3. Nuclei were stained with Hoechst. Representative images of one of the brain sections with similar results in each case is shown.

neurons were treated with Aβ, and cell lysates were immunoprecipitated with Trib3 antibody and Western blotted with Akt antibody and vice versa. Results revealed increased binding of Trib3 with Akt in Aβ-treated neurons compared with control neurons (Fig. 3, *A* and *B*). We then checked the phosphorylation status of Akt upon Aβ treatment. We observed that the decrease in phosphorylation at Ser-473 of Akt caused by Aβ insult was rescued when Trib3 was down-regulated (Fig. 3, *C* and *D*). We also observed that when PI3K is inhibited by a specific PI3K inhibitor in the presence or absence of Aβ, the protein levels of Trib3 increased even in the absence of Aβ (Fig. 3, *E* and *F*). This allowed us to see whether Trib3 is regulated by some downstream substrate of PI3K/Akt, which gets activated upon PI3K inhibition and in turn regulates Trib3. Transcription factor FoxO, downstream to PI3K/AKT and an entrenched substrate of it, is known to translocate from the cytosol to

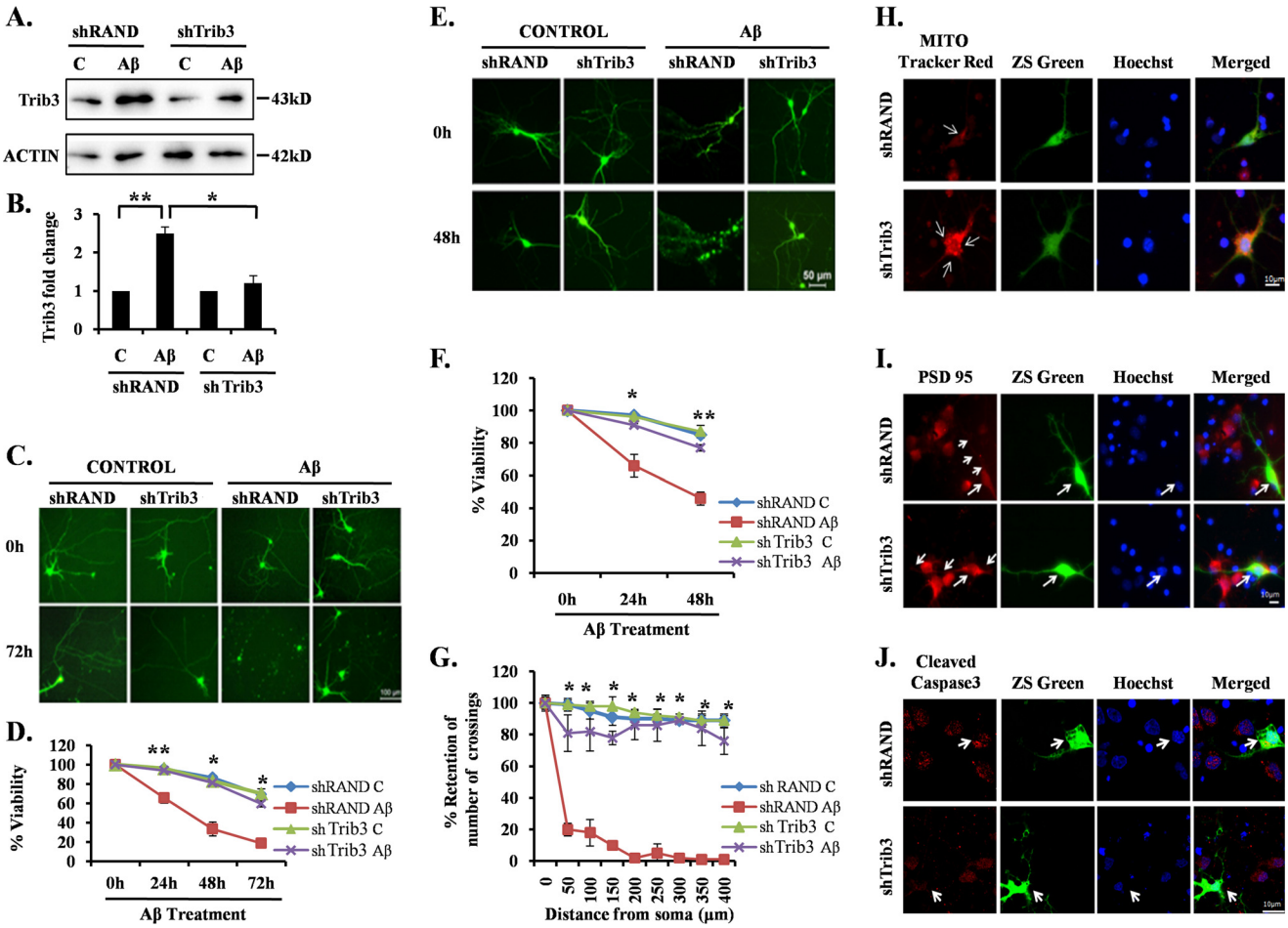

FIGURE 2. **Trib3 is essential for neuronal death evoked by Aβ.** *A,* PC12 cells were transfected with shTrib3 or shRand, primed, and then treated with and without Aβ (5 μM). Levels of endogenous Trib3 levels were assessed by Western blotting analysis using anti-Trib3 antibody. *Lane C,* control. *B,* graphical representation of fold change of Trib3 levels by densitometric analysis of Western blottings. Data represent mean ± S.E. of three independent experiments. *, $p < 0.05$; **, $p < 0.005$. Primary cultured rat cortical neurons (5DIV) (*C*) and primary cultured hippocampal neurons (19DIV) (*E*) were transfected with pSIREN-shTrib3-zsgreen (shTrib3) or control pSIREN-shRand-zsgreen (shRand) and maintained for 48 h and then subjected to Aβ (1.5 μM) treatment for 72 h. Representative pictures of transfected neurons that were maintained in the presence or absence of Aβ for the indicated time periods are shown. Images were taken using an inverted fluorescence microscope. *D* and *F,* graphical representation of percentage of viable green cells after each time point. Numbers of surviving transfected (*green*) cells were counted under fluorescence microscope just before Aβ treatment and after 24, 48, and 72 h of the same treatment. Data are from three independent experiments, each with comparable results, and are shown as mean ± S.E., performed in triplicate. The *asterisks* denote statistically significant differences from control (shRand) at corresponding time points: *, $p < 0.05$; **, $p < 0.001$. *G,* Trib3 knockdown prevents neuronal degeneration and preserves neuritic processes. Sholl analysis of single imaged neurons by using ImageJ was done as described under "Experimental Procedures." Data represent mean ± S.E. of six different neurons from three independent cultures for each class. *Asterisks* denote statistically significant differences from shRand (control): *, $p < 0.001$. *H–J,* cultured cortical neurons (5DIV) were transfected with shTrib3 and shRand, and the cells were maintained for the next 48 h and then treated with 1.5 μM Aβ for 16 h, after which they were immunostained with MitoTracker red dye (*H*), PSD95 (*I*), or cleaved caspase3 antibodies (*J*).

nucleus and induces its target genes in Aβ-treated neurons (38, 44). Previous reports reveal the presence of putative FoxO-binding sites on the *Trib3* promoter (45–48). We therefore hypothesized that Trib3 may be regulated by FoxO transcription factors in Aβ-treated neurons. We performed chromatin immunoprecipitation assay to check the direct binding of FoxO1 with the *Trib3* promoter. The result showed that FoxO1 occupancy of the *Trib3* promoter was markedly increased in response to Aβ (Fig. 3, *G* and *H*). These results indicate that Trib3 directly binds and inactivates Akt; this in turn activates the transcription factor FoxO1, and FoxO1 can occupy the *Trib3* gene promoter upon Aβ treatment.

Feed-forward Regulatory Mechanism Acts between Trib3 and FoxO1—Previous results prompted us to test whether a feed-forward regulatory mechanism acts between Trib3 and FoxO in neuronal cells in response to Aβ insult. To study the regulation of Trib3 by FoxO, we knocked down the FoxOs in cortical neurons by a previously reported shRNA that targets all FoxO isoforms (49) and exposed them to Aβ and performed immunocytochemistry to see the endogenous Trib3 expression. Results revealed that the shRNA-mediated knockdown of FoxOs led to reduced expression of Trib3 in most of the transfected cells compared with non-transfected neighboring cells upon exposure of Aβ (Fig. 4*A*). In contrast, no such reduction on Trib3 expression was found in shRand-transfected cells (Fig. 4*A*). A quantitative analysis showed that about 80% shFoxO and about 20% shRand-transfected neurons had reduced Trib3 levels upon Aβ treatment (Fig. 4*B*). To confirm this result, we performed a Western blotting analysis of Aβ-treated shFoxO and shRand-transfected cells, and we observed the Trib3 protein levels. We observed that down-regulating FoxOs blocked induction of Trib3 protein caused

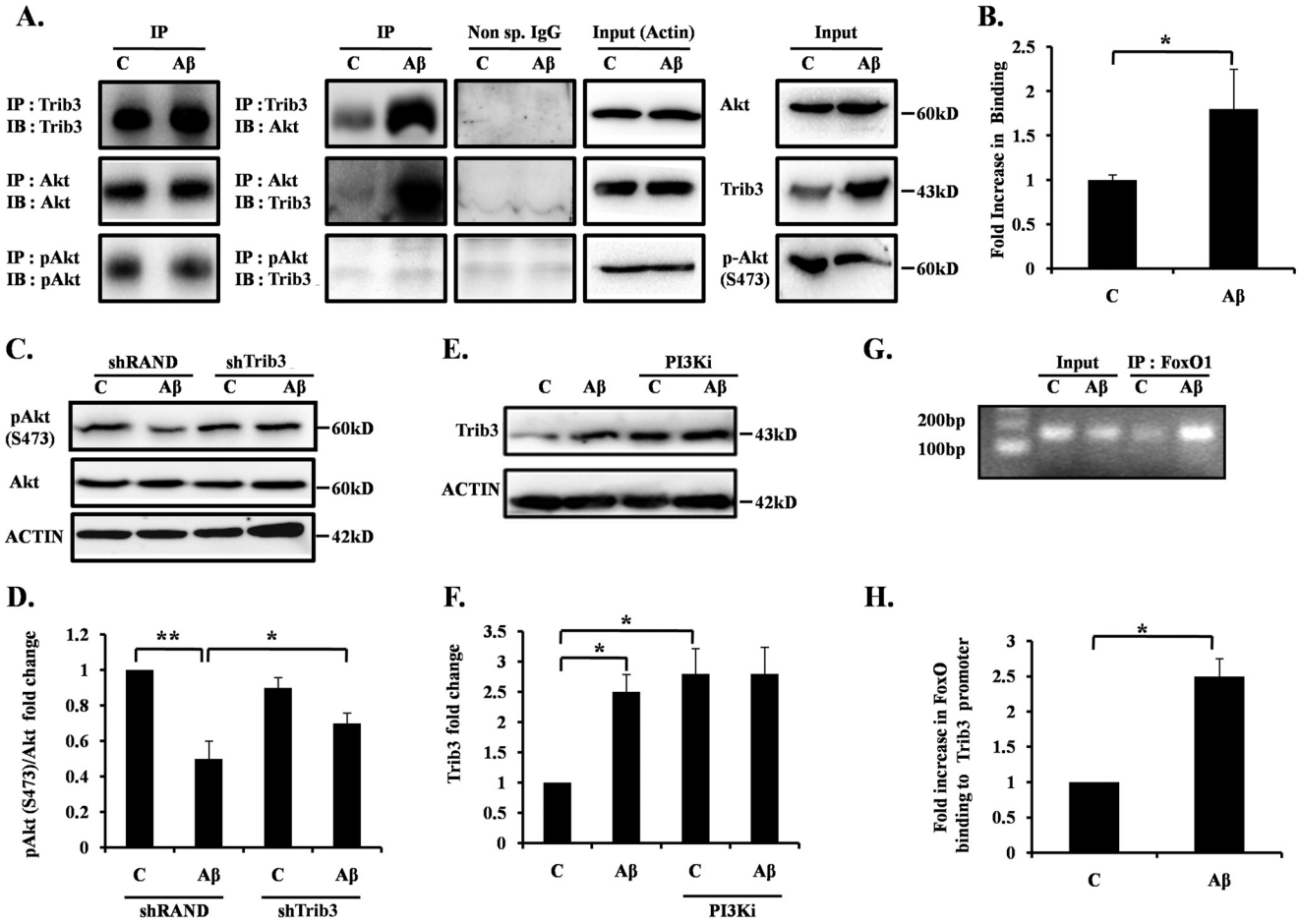

FIGURE 3. **Trib3 binds to Akt and negatively regulates it.** *A,* cultured rat cortical neurons were treated with 1.5 μM Aβ for 16 h; cell lysate was immunoprecipitated (*IP*) with Trib3 antibody and immunoblotted (*IB*) with Akt antibody; reverse immunoprecipitation was also performed to check interaction of Trib3 with Akt; cell lysate was also immunoprecipitated with p-Akt and immunoblotted with Trib3 (*2nd column*). Immunoprecipitation with nonspecific antibody was done to check specificity of the reactions (*3rd column*). Actin was used as loading control (*4th column*). Levels of the specific proteins in cell lysates (*Inputs*) were also checked (*5th column*). Immunoblot of the respective immunoprecipitated protein was also performed (*1st column*). *Lane C*, control. *B,* graphical representation of the Akt protein levels as quantified by densitometry of Western blottings. Data represents mean ± S.E. of three independent experiments. *, $p < 0.05$. *C,* primed PC12 cells were transfected with shTrib3 or shRand, treated with and without Aβ 5 μM. Levels of endogenous p-Akt(Ser-473) were assessed by Western blotting analysis using anti-p-Akt(Ser-473) antibody. *D,* graphical representation of fold change of p-Akt(Ser-473) levels by densitometric analysis of Western blottings. Data represent mean ± S.E. of three independent experiments. *, $p < 0.05$; **, $p < 0.005$. *E,* cultured cortical neurons were treated with Aβ 1.5 μM for 16 h, with and without LY 294002 (*PI3Ki*). Total cell lysates were subjected to Western analysis with Trib3 antibody. A representative immunoblot of three independent experiments with similar results is shown. *F,* graphical representation of fold change of Trib3 upon Aβ treatment with and without PI3Ki. Data represent mean ± S.E. of three independent experiments. *, $p < 0.05$. *G,* primary cultures of rat cortical neurons were treated with or without Aβ for 8 h. An equal number of cells were processed for ChIP assay using anti-FoxO1 antibody for immunoprecipitation. The immunoprecipitated materials were subjected to PCR using primers against the region of *Trib3* promoter that contains the putative FoxO1-binding site. PCR products were verified by agarose gel electrophoresis. Templates were DNA from cells before ChIP (*input*) or DNA from immunoprecipitated (*IP*) materials. PCR assays were conducted after ChIP using samples from cells that were either left untreated (control) or treated with Aβ. ChIP assay indicates that FoxO1 occupancy of rat *Trib3* promoter regions enhances after Aβ exposure. *H,* graphical representation of fold changes in FoxO1 association with the *Trib3* promoter upon Aβ treatment. Data represent mean ± S.E. of three independent experiments. *, $p < 0.05$.

by Aβ toxicity (Fig. 4, *C* and *D*). This indicates that FoxOs act as regulator of Trib3.

Next, we investigated whether Trib3 regulates FoxO1 in our model. Cortical neurons were transfected with shTrib3, treated with Aβ and immunostained to study FoxO1 expression. It has already been reported that nuclear translocation of FoxO1 is controlled by Trib3 in anti-NGF-treated neurons (23). In our study we found that shTrib3 not only blocked translocation of FoxO1 but also reduced its protein levels (Fig. 4, *E* and *F*). To confirm our result, we transfected neuronal PC12 cells with shTrib3 and shRand, treated with Aβ for 16 h, and performed Western blotting analysis for FoxO1 protein. Results confirmed that down-regulation of Trib3 led to reduced levels of FoxO1 in the presence or absence of Aβ (Fig. 4, *G* and *H*). Thus, our findings indicate that Trib3 regulates both the level and activity of FoxO1 following Aβ treatment. Collectively, these results suggest a feed-forward loop that involves inhibition of Akt by Trib3, activation of transcription factor FoxO1 upon inactivation of Akt, and transactivation of Trib3 by FoxO1 in Aβ-treated neurons.

Trib3 Further Downstream Regulates Pro-apoptotic Gene Bim in Neuronal Cell Death Induced by Aβ—It has also been reported that transcription factor FoxO regulates Bim upon NGF deprivation in sympathetic neurons (50). We have recently shown that Bim is directly regulated by FoxO in neurons following Aβ treatment (38). We therefore determined whether Bim is under the control of Trib3 in this death paradigm. We transfected cultured cortical neurons with shTrib3 or

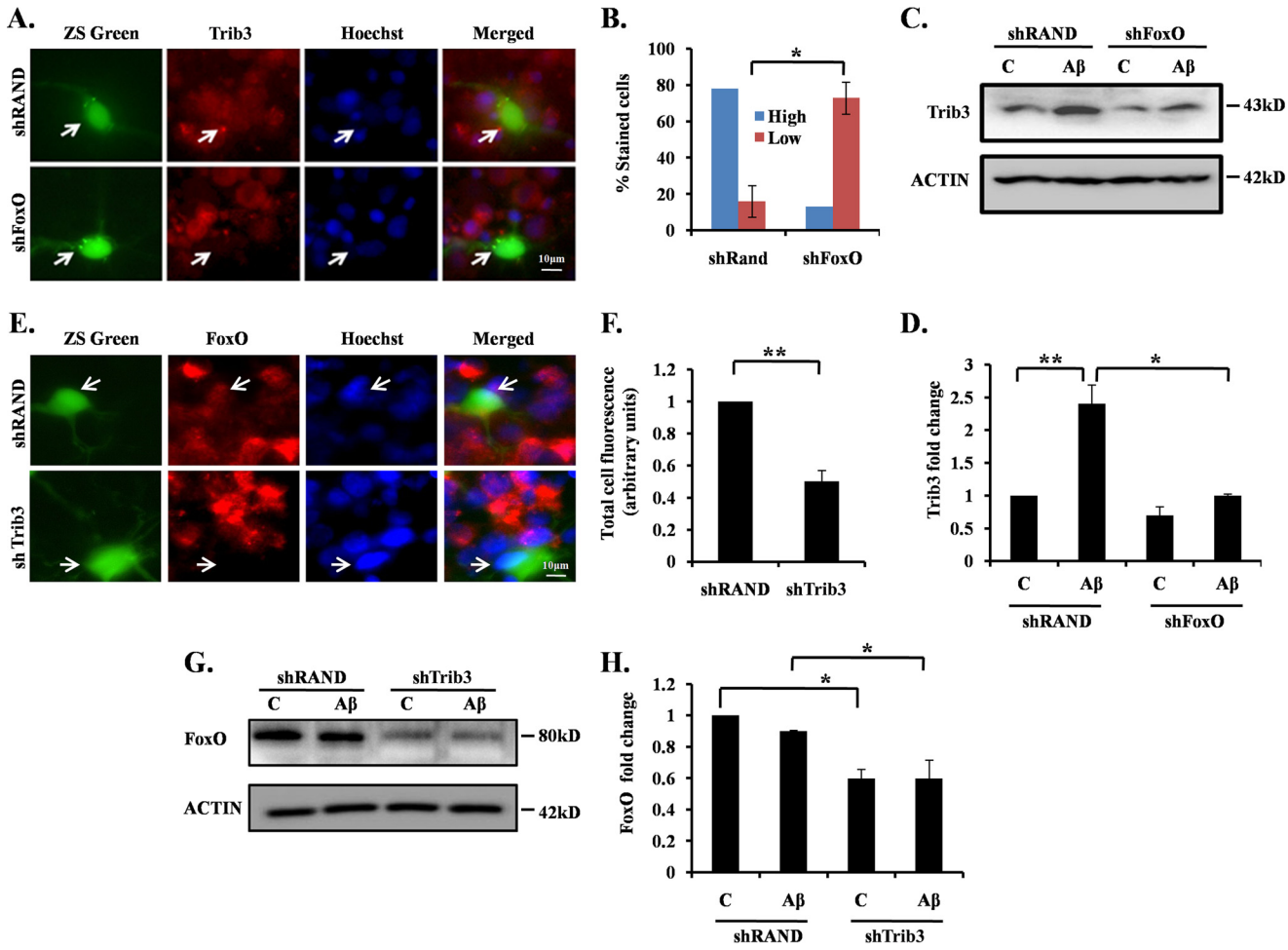

FIGURE 4. **Feed-forward loop acts between Trib3 and Akt upon Aβ exposure.** *A,* cultured cortical neurons at 5DIV were transfected with shFoxO or shRand, treated with 1.5 μM Aβ for 16 h, and immunostained with Trib3 antibody. *B,* percentage of stained cells indicate the proportions of transfected cells (*green*) with high (more or equal than the neighboring non-transfected cells) or low (less than the neighboring non transfected cells) Trib3 immunoreactivity levels after treatment with Aβ. Data represent mean ± S.E. of three experiments. Number of cells evaluated per culture are 50 (approximate). *, $p < 0.01$. *C,* PC12 cells were transfected with shFoxO or shRand, primed, and then treated with 5 μM Aβ for 16 h. The down-regulation of endogenous Trib3 was analyzed by Western blotting with anti-Trib3 antibody. *Lane C,* control. *D,* graphical representation of fold change of Trib3 levels by densitometric analysis upon transfection with shFoxO or shRand in the presence or absence of Aβ 5 μM. Data represent mean ± S.E. of three independent experiments. *, $p < .05$; **, $p < 0.001$. *E,* cultured cortical neurons were transfected with shRand and shTrib3, maintained for 48 h, then treated with Aβ 1.5 μM. Immunocytochemical staining was performed with FoxO1 antibody. *F,* graphical representation of corrected total cell fluorescence of FoxO1 in neurons transfected with shRand or shTrib3 following Aβ exposure. Difference in intensity of FoxO1 staining is quantified by ImageJ as described under "Experimental Procedures." Data represent mean ± S.E. of 30 different cells from three independent experiments. **, $p < 0.001$. *G,* PC12 cells were transfected with shTrib3 or shRand, primed, and then treated with 5 μM Aβ for 16 h. Down-regulation of endogenous FoxO1 was assessed by Western blotting analysis with anti-FoxO1 antibody. *H,* graphical representation of fold change of FoxO1 levels by densitometric analysis upon transfection with shTrib3 or shRand in the presence or absence of Aβ. Data represent mean ± S.E. of three independent experiments. *, $p < 0.05$.

shRand and exposed them to Aβ followed by immunocytochemical analysis for Bim expression. Results revealed that down-regulating Trib3 resulted in a marked reduction of Bim expression, as evident from reduced Bim staining in shTrib3-transfected cells as compared with shRand-transfected cells (Fig. 5, *A* and *B*). To further corroborate our findings, we performed Western blotting analysis with Trib3 knockdown PC12 cells for Bim levels following Aβ treatment. We observed a significant up-regulation of Bim following Aβ exposure in shRand-transfected cells as expected. But interestingly, this up-regulation was significantly blocked in shTrib3-transfected cells even after Aβ treatment (Fig. 5, *C* and *D*). These findings thus indicate that Trib3 induces neuronal death upon Aβ exposure by activating Bim, which could be via the Akt-FoxO1 pathway.

Trib3 Induces Autophagy in Neurons via the Akt-mTOR Pathway—Recently, it has been reported that Trib3 induces autophagy in cancer cells in response to cannabinoid by inhibiting the Akt/mTORC1 axis (14, 15). Multiple studies implicate impaired autophagy in the pathogenesis of AD (9–13). Aβ treatment can induce both apoptosis and autophagy in neuronal cells (data not shown) (10, 12, 35, 51). Therefore, we investigated whether Trib3 also induces autophagy in Aβ-treated neuronal cells. We transfected differentiated PC12 cells with shTrib3 or shRand and followed it with Aβ treatment. Western blotting analysis was performed to check the level of phospho-mTOR at Ser-2448 (p-mTOR) and total mTOR. We observed that upon treatment, p-mTOR levels decrease, and this decrease in phosphorylation level can be blocked by down-regulating Trib3 (Fig. 6, *A* and *B*). A direct target of

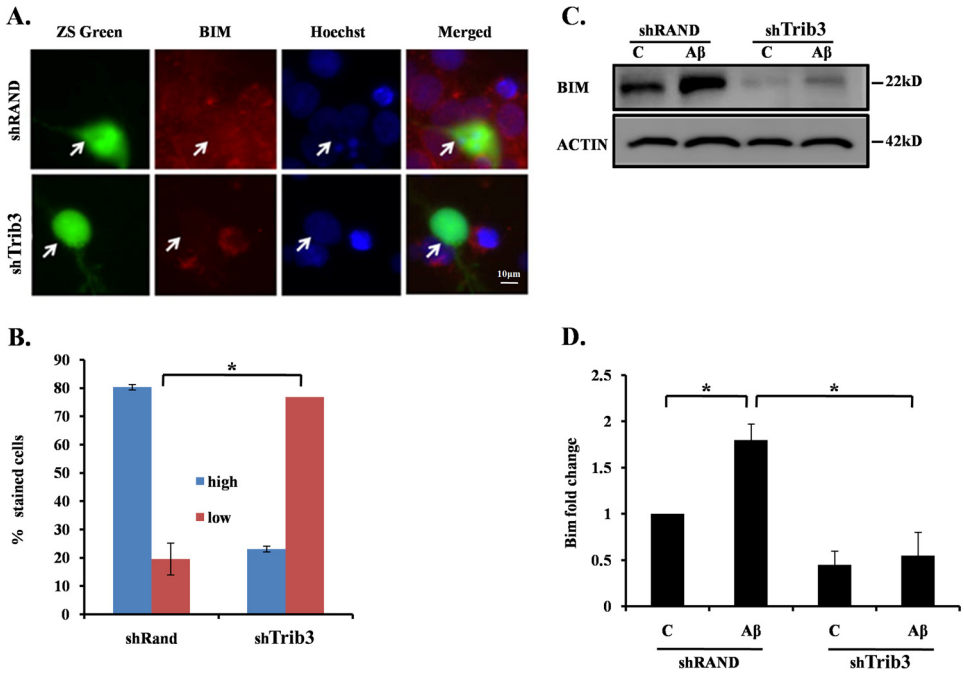

FIGURE 5. **Upon Aβ exposure Trib3 leads to apoptotic death of neurons via Bim.** *A,* cultured cortical neurons (5DIV) were transfected with shTrib3 and shRand, and the cells were maintained for the next 48 h and then treated with Aβ 1.5 μM for 16 h, after which they were immunostained with Bim antibody (*red*). *B,* percentage of stained cells indicates the proportions of transfected cells (*green*) with high (more or equal than the neighboring non-transfected cells) or low (less than the neighboring non transfected cells) Bim immunoreactivity levels after treatment with Aβ. Data represent mean ± S.E. of three experiments. Number of cells evaluated per culture are 50 (approximate). The *asterisk* denotes statistically significant differences between low staining cells and high staining cells: *, $p < 0.01$. *C,* PC12 cells were transfected with shTrib3 or shRand, primed, and then treated with 5 μM Aβ. Down-regulation of endogenous Bim levels was analyzed by Western blotting using Bim antibody. *Lane C*, control. *D,* graphical representation of fold change of Bim levels by densitometric analysis upon transfection with shTrib3 or shRand in the presence or absence of Aβ 5 μM. Data represent mean ± S.E. of three independent experiments. *, $p < 0.05$.

p-mTOR is Ulk1 (52). mTOR when phosphorylated leads to the inactivating phosphorylation of Ulk1 at Ser-757. This results in reduced autophagy. We therefore analyzed the phosphorylation status of the Ulk1 protein. We found that Ulk1 phosphorylation at Ser-757 was reduced upon Aβ treatment and rescued by down-regulating Trib3 (Fig. 6, *C* and *D*). Analysis of pUlk1 levels in transgenic mice revealed that there is decreased expression of pUlk1(Ser-757) in the transgenic mouse brain as compared with the brain of wild type (Fig. 6, *E* and *F*). Taken together, these results indicate that Trib3 when induced upon Aβ treatment leads to enhanced levels of autophagy by inhibiting mTOR and activating Ulk1 activity.

Trib3 Induces Frustrated Autophagy in Neurons—Although a basal level of autophagy is required for protein degradation and organelle turn over, reports indicate that increased autophagy facilitates enhanced clearance of aggregated proteins, thus promoting survival of neurons (11, 12). However, if there is an incessant up-regulation of autophagic activity, it can lead to cell death (53). Autophagic death is said to occur not just due to increased autophagosome formation but also when there is a dysregulation of autophagic flux. Such an autophagy is referred to as frustrated autophagy (54). To check the efficiency of autophagy induced by Trib3, we monitored the levels of LC3 after Aβ exposure. We found that upon Aβ exposure there was an increase in LC3 punctate staining in transgenic mouse brain sections as compared with wild-type mice (Fig. 6, *G* and *H*). The levels of both LC3-I and LC3-II in the cells have also increased in response to Aβ treatment (Fig. 6, *I* and *J*). However, there was a significant reduction in the levels of LC3-II when Trib3 was down-regulated (Fig. 6, *I–L*). It has been reported that p62 is accumulated when autophagic degradation is inhibited and is therefore considered a marker of autophagy flux (55, 56). We checked the autophagy flux in Aβ-treated cells by monitoring p62 levels. Interestingly, we found that there was an increased accumulation of p62 in the transgenic mouse brain as compared with the wild-type mouse brain (Fig. 7, *A* and *B*). The level of p62 was also increased in cells treated with Aβ (data not shown). Conversely, the increase in p62 levels in these cells was blocked when Trib3 was down-regulated (Fig. 7, *C–F*). In contrast, when Trib3 was overexpressed, an enhanced accumulation of p62 was observed in the cells (Fig. 7, *G* and *H*). Collectively, these results indicate that Trib3 induces autophagy in Aβ-treated cells. However, it culminates in a frustrated autophagy due to decreased autophagic flux as seen by accumulation of p62.

Aβ-induced Impaired Autophagy Flux Contributes to Neuron Death—Our results suggest that Trib3 up-regulation upon Aβ exposure leads to induction of both apoptosis and autophagy. We determined the contribution of these two processes on neuron death evoked by Aβ. We found that inhibition of both these processes separately blocks the death of neuronal PC-12 cells substantially. Moreover, inhibition of both apoptosis and autophagy provided better protection to these cells from Aβ toxicity (Fig. 8, *A* and *B*). Thus, our results suggest that simultaneous induction of apoptosis and autophagy by Aβ leads to neuronal cell death.

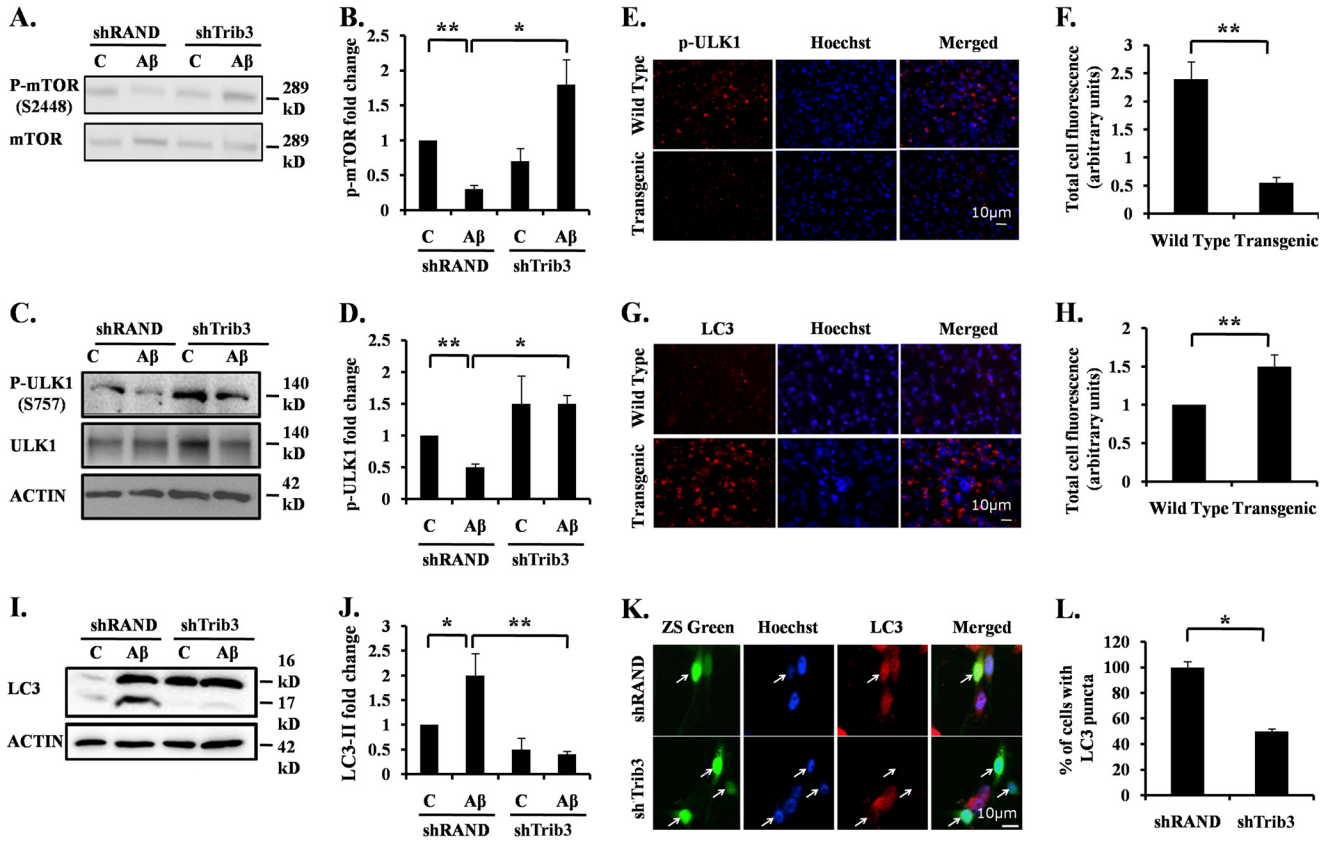

FIGURE 6. **Trib3 leads to increased autophagy in neuronal cells upon Aβ exposure.** *A,* differentiated PC12 cells were transfected with shTrib3 or shRand, primed, and then treated with 5 μM Aβ. Phosphorylation status of mTOR at Ser-2448 was analyzed by Western blotting of cell lysate using p-mTOR antibody, total level of mTOR was also checked. *Lane C*, control. *B,* graphical representation of fold change of p-mTOR level by densitometric analysis upon transfection with shTrib3 or shRand in presence or absence of 5 μM Aβ. Data represent mean ± S.E. of three independent experiments. *, $p < 0.05$; **, $p < .001$. *C,* PC12 cells were transfected with shTrib3 or shRand, primed, and then treated with 5 μM Aβ. Phosphorylation status of Ulk1 was analyzed by Western blotting using P-Ulk1 antibody; total level of Ulk1 was also checked. *D,* graphical representation of fold change of P-Ulk1 level by densitometric analysis upon transfection with shTrib3 or shRand in presence or absence of 5 μM Aβ. Data represent mean ± S.E. of three independent experiments. *, $p < 0.05$; **, $p < .001$. *E,* brain sections obtained from AβPPswe-PS1de9 transgenic mice and control littermates were stained with p-ULK1 (Ser-757) antibody. Nuclei were stained with Hoechst. Representative image of one of the brain sections with similar results in each case is shown. *Lane C*, control. *F,* graphical representation of corrected total cell fluorescence of pUlk1 in transgenic and wild-type brain sections. Difference in intensity of pUlk1 staining is quantified by ImageJ as described under "Experimental Procedures." Data represent mean ± S.E. of 30 different cells from three independent experiments. **, $p < 0.001$. *G,* brain sections obtained from AβPPswe-PS1de9 transgenic mice and control littermates were stained with LC3 antibody. Nuclei were stained with Hoechst. Representative image of one of the brain sections with similar results in each case is shown. *H,* graphical representation of corrected total cell fluorescence of LC3 in transgenic and wild-type brain sections. Difference in intensity of LC3 staining is quantified by ImageJ as described under "Experimental Procedures." Data represent mean ± S.E. of 30 different cells from three independent experiments. **, $p < 0.001$. *I,* PC12 cells were transfected with shTrib3 or shRand, and cells were primed and treated with 5 μM Aβ for 24 h. Cleaved levels of LC3 were analyzed by Western blotting using LC3 antibody. *J,* graphical representation of fold change of LC3-II levels by densitometric analysis upon transfection with shTrib3 or shRand in presence or absence of 5 μM Aβ. Data represent mean ± S.E. of three independent experiments. *, $p < 0.05$; **, $p < .001$. *K,* cultured cortical neurons (5DIV) were transfected with shTrib3 and shRand; the cells were maintained for the next 48 h and then treated with 1.5 μM Aβ for 16 h, after which they were immunostained with LC3 antibody (*red*). *L,* graphical representation of percentage of cells expressing LC3 puncta. Data represent mean ± S.E. of 30 different cells from three independent experiments. *, $p < 0.05$.

Discussion

In this study, we investigated the role of Trib3 in Aβ-induced neurodegeneration. A number of our experimental observations indicate that Trib3 promotes neuronal death by both apoptosis and autophagy in response to Aβ. We found that Trib3 expression is up-regulated in neuronal cells both at transcriptional and translational levels following Aβ treatment. A similar induction of Trib3 was also found in the Aβ-infused rat model. Because we used synthetic Aβ for our experiments, which could have disparate effects from the naturally occurring Aβ, we also examined the induction of Trib3 in the transgenic mouse brain that overexpresses human Aβ. The result from these transgenic mice also showed an elevated level of Trib3 protein corroborating our previous *in vitro* results. Moreover, knocking down Trib3 by using shRNA in cortical or hippocampal neurons protects cells from Aβ-induced cell death. Sholl analysis further exhibits the retention of neuronal processes as well as preservation of the overall neuronal morphology in Trib3 knocked down neurons, even after Aβ treatment.

An important question is how Aβ applied in media affects different organelles in the cells. Reports suggest that Aβ from the medium is internalized by the PC12 cells, enters their nuclei (57), and leads to death of PC12 cells (58). Studies also reveal that Aβ enters neurons and is present in their lysosomal system (59), whereas inhibition of its engulfment reduces death of neurons (60). Aβ immunoreactivity has also been found in degenerating neurons in transgenic mice and AD brains (61, 62).

Mechanistic studies reveal that Trib3 interacts and negatively regulates survival kinase Akt. These results corroborate previous results whereby overexpression of Trib3 reduced phos-

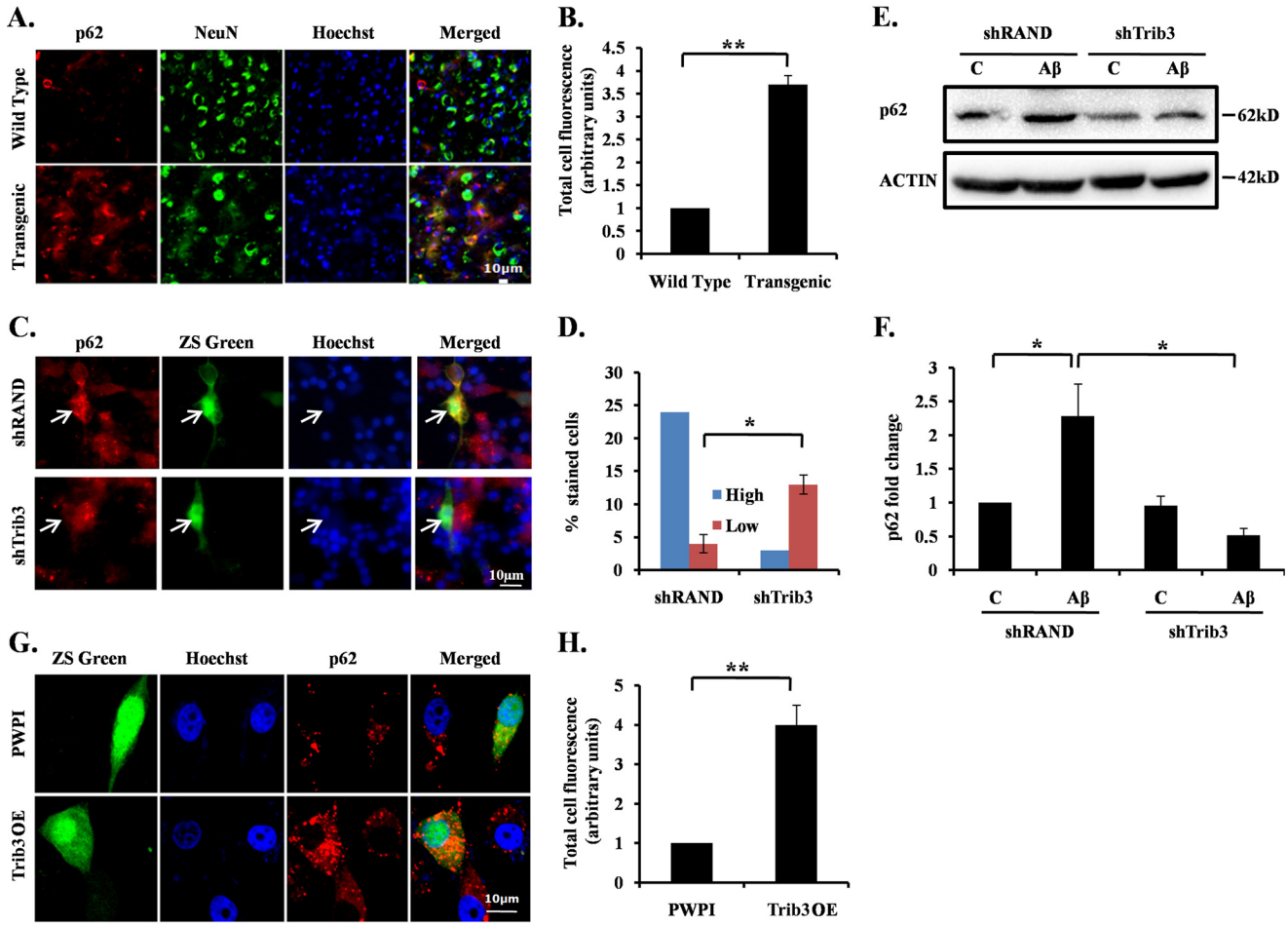

FIGURE 7. **Aβ induces frustrated autophagy in neurons.** *A,* brain sections obtained from AβPPswe-PS1de9 transgenic mice and control littermates were stained with p62 antibody. Nuclei were stained with Hoechst. Representative image of one of the brain sections with similar results in each case is shown. *B,* graphical representation of corrected total cell fluorescence of p62 in transgenic and wild-type brain sections. Difference in intensity of p62 staining is quantified by ImageJ as described under "Experimental Procedures." Data represent mean ± S.E. of 30 different cells from three independent experiments. **, $p < 0.001$. *C,* cortical neurons were transfected with shTrib3 or shRand, and 48 h post-transfection they were treated with 1.5 μM Aβ. p62 levels were determined by immunocytochemical staining using p62 antibody. *D,* percentage of stained cells indicates the proportions of transfected cells (*green*) with high (more or equal than the neighboring non-transfected cells) or low (less than the neighboring non transfected cells) p62 immunoreactivity levels after treatment with Aβ. *, $p < 0.05$. *E,* PC12 cells were transfected with shTrib3 or shRand, primed, and then treated with 5 μM Aβ. Levels of p62 were analyzed by Western blotting using p62 antibody. *F,* graphical representation of fold change of p62 levels by densitometric analysis upon transfection with shTrib3 or shRand in presence or absence of Aβ 5 μM. Data represents mean ± S.E. of three independent experiments. *, $p < 0.05$. *G,* primed PC12 cells were transfected with Trib3 overexpression vector or PWPI as control. 48 h post-transfection cells were fixed, and p62 levels were checked by immunocytochemical staining using p62 antibody. *H,* graphical representation of corrected total cell fluorescence of p62 in differentiated PC12 cells transfected with PWPI or Trib3 OE vector. Difference in intensity of p62 staining is quantified by ImageJ as described under "Experimental Procedures." Data represent mean ± S.E. of 30 different cells from three independent experiments. **, $p < 0.001$.

phorylation of Akt at Ser-473 and Thr-308 (23) and knockdown of Trib3 restored phosphorylation of Akt in tunicamycin-treated PC12 cells (28). Interestingly, it has recently been shown that Trib3 induction, Akt inhibition, and FoxO activation are linked in a self-amplifying loop that culminates in neuron death evoked by NGF deprivation (23). We have also found that inhibition of PI3K/Akt signaling by LY294002 led to up-regulation of Trib3. In recent years, FoxO transcription factors have been shown to play an important role in neurodegeneration (38, 44). Reports suggest putative FoxO-binding sites on the *Trib3* promoter (45–48). Our results revealed an enhanced occupancy of FoxO1 on the *Trib3* gene that regulated its expression upon Aβ insult. These findings clearly indicate that a feed-forward regulatory mechanism is active between Trib3, Akt, and FoxO1 in Aβ-treated neuronal cells as well. Next, we investigated the downstream target of up-regulated Trib3 that mediates neuronal death. We observed that down-regulating Trib3 abrogates the up-regulation of Bim upon Aβ exposure suggesting the potential role of Bim in the mechanism by which Trib3 synchronizes apoptotic death of neurons. Bim is a FoxO target and has also been implicated in neuronal apoptosis in AD (49, 63–65).

Interestingly, we found that neuronal death caused by Trib3 overexpression could not be fully rescued by inhibiting caspases.[3] This aroused our curiosity to investigate the possibility of the existence of a varied mechanism by which Trib3 could be triggering cell death. Reports revealed that Trib3 was responsible for autophagic death in cancer cells (6, 7, 14). Autophagic failure in AD has also been studied extensively

[3] S. Saleem and S. C. Biswas, unpublished observations.

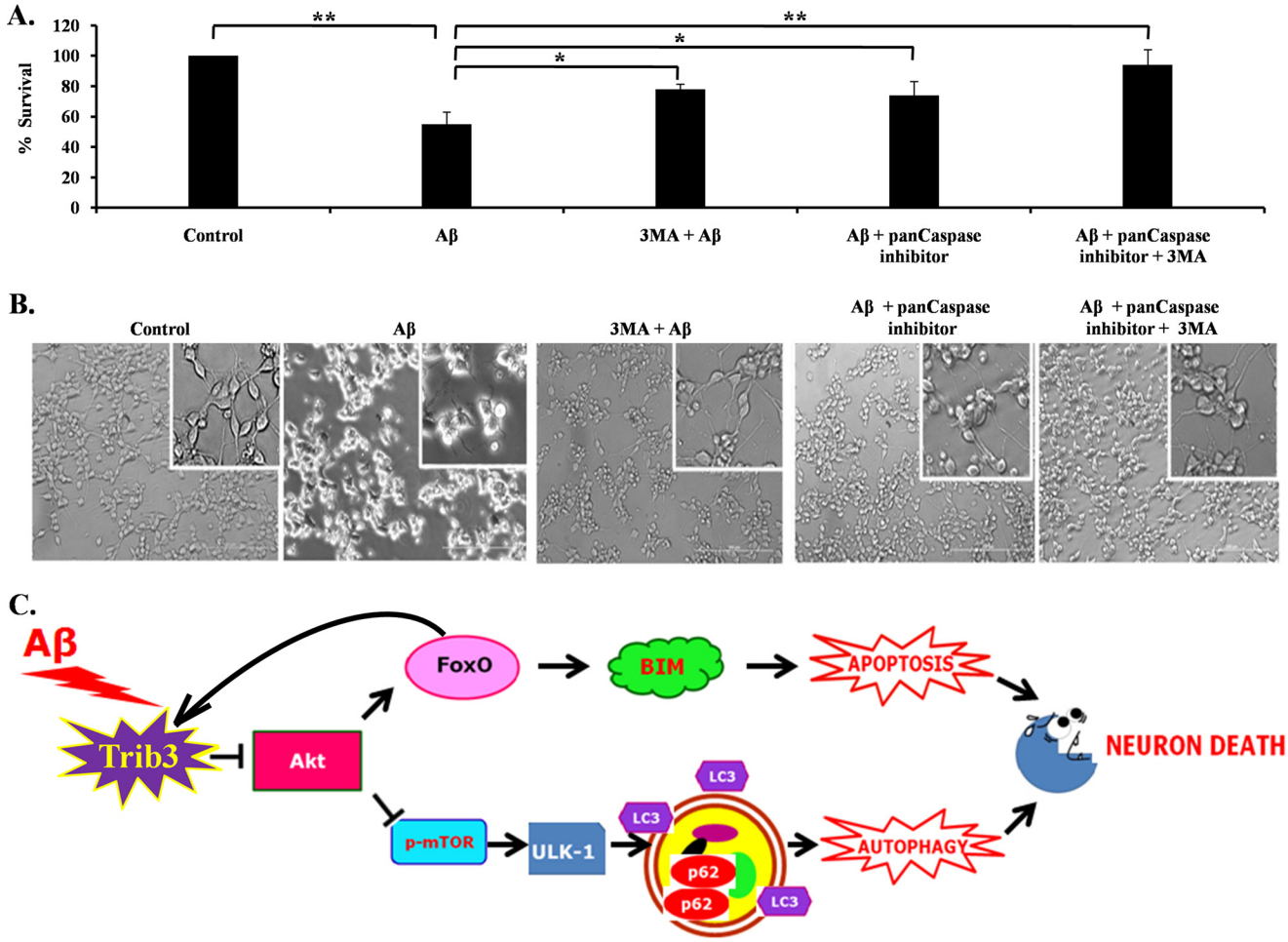

FIGURE 8. **Contribution of both autophagy and apoptosis in Aβ-induced neuronal cell death.** *A,* graphical representation of cell survival following Aβ treatment with pan-caspase inhibitor and 3-methyladenine (*3-MA*), or both, for 16 h. Data are represented as mean ± S.E. of three independent experiments. *, $p < 0.05$; **, $p < 0.001$. *B,* representative phase contrast micrographs of neuronal PC12 cells before and after treatment of Aβ for 16 h. *C,* Trib3 is up-regulated upon Aβ exposure, Trib3 then interacts with Akt and inhibits its phosphorylation, as a result of which two molecules are affected. On the one hand, FoxO gets activated, translocates to the nucleus, and causes transcription of the pro-apoptotic protein Bim; FoxO also binds to the promoter region of *Trib3* amplifying the feed-forward loop between them. On the other hand, mTOR gets inhibited, as a result of which Ulk1 is activated which then initiates the autophagic cascade as seen by the induction of cleavage of LC3 and increased accumulation of p62. Trib3 thus designs death of neurons by both autophagy and apoptosis.

(66–69). mTOR is the master regulator of autophagy (52, 70). The signaling cascade PI3K/Akt/mTOR is inhibited by Aβ (71). Trib3 inhibits the Akt/mTOR axis and leads to autophagy in human glioma cells (7). In corroboration with previous reports, we also found that Aβ induces dephosphorylation of mTOR and inactivates it. Down-regulating Trib3 blocked the dephosphorylation of mTOR after Aβ treatment. Moreover, we also observed that Ulk1, a direct target of mTOR, is activated upon Aβ treatment, which is required to initiate the autophagic cascade. Furthermore, we found an elevated level of the autophagosome marker LC3 in AD transgenic mice. Interestingly, down-regulating Trib3 blocked the activation of Ulk1 and demolished the increase in LC3 II upon Aβ treatment. This affirms the fact that Trib3 plays a critical role in Aβ-induced autophagy. Furthermore, Trib3 regulates autophagy flux as well. We checked an important marker for autophagy flux, p62. In conditions of frustrated autophagy when the vacuoles are unable to fuse with the lysosomes, or when there is abnormal clearance of these vacuoles, there occurs accumulation of p62 within the cell (56). We observed that upon Aβ treatment there was an accumulation of p62; down-regulation of Trib3 abrogated this induction, and overexpressing Trib3 increases its accumulation. It has recently been reported that accumulation of p62 can mediate apoptosis via caspase-8 (72). However, accumulating evidence indicates that high levels of autophagy can lead to autosis, which is an autophagy-dependent non-apoptotic cell death (73, 74). This suggests that Trib3 could also be involved in autophagic death induced by Aβ by increasing the aggregation of autophagic vacuoles with decreased clearance from the cells. The critical role of FoxO proteins in inducing autophagy in cardiomyocytes, hepatocytes, and skeletal muscles has also been well studied (75–78). The exact mechanism by which Trib3 and FoxO together orchestrate autophagy in neurons still remains to be clearly elucidated.

Conclusions

Taken together, our results suggest a model in which Trib3 is involved in causing death of neurons treated with Aβ by a dual modality, whereby it induces apoptosis and also up-regulates autophagy with defective autophagic flux (Fig. 8*C*). Autophagic

dysfunction is a multidimensional anomaly, identifying the exact nature of the defect is of utmost importance for therapeutic intervention (67). The signal that promotes apoptosis could also activate autophagy (79). Both apoptosis and autophagy are dysregulated in several neurodegenerative disorders, and there occurs an obscure cross-talk between the two phenomena (80, 81). Our findings bring to light Trib3 as the molecule, which, via Akt, designs neuronal death paradigm by apoptosis and autophagy. We anticipate that Trib3 could act as a potential target for therapeutic intervention in AD.

Experimental Procedures

Materials—Aβ(1–42) was purchased from American Peptide. TRI Reagent, 1,1,1,3,3,3-hexafluoro-2-propanol (HFIP), insulin, progesterone, transferrin, NGF, poly-D-lysine, putrescine, selenium, *In situ* cell death detection kit, rapamycin, and 3-methyladenine were purchased from Sigma. Anti-FoxO1, cleaved anti-LC3, anti-Akt, anti-p-Akt(Ser-473), anti-p-mTOR (Ser-2448), anti-mTOR, anti-p-ULK1 (Ser-757), active caspase-3, and anti-ULK1 antibodies were from Cell Signaling Technology (Danvers, MA). Anti-LC3 antibody (Novus), anti-Trib3 antibody, pan-caspase inhibitor, and LY 294002 were purchased from Calbiochem; anti-p62 antibody was purchased from R&D Systems (Minneapolis, MN); anti-Bimand anti-Aβ antibodies were from Abcam (Cambridge, UK). Protein A-agarose and HRP-conjugated secondary antibodies were from Santa Cruz Biotechnology (Dallas, TX). Lipofectamine 2000, Alexa Fluor 488, Alexa Fluor 568, culture media, and serum were purchased from Invitrogen. PSD-95 antibody was obtained from Neuromab (University of California at Davis, Davis, CA). MitoTracker Red was from Thermo Fisher Scientific (Waltham, MA). Brain tissues of APPswe-PS1de9 mice and control littermates were kindly gifted by Dr. Anant B. Patel (Council of Scientific and Industrial Research-CCMB, Hyderabad, India). Male mice, about 12 months old, were used for the study.

Cell Culture—Cortical neurons from the neocortex of E18-day embryonic rat brains were cultured as described previously (82). The cells were plated on poly-D-lysine-coated culture plates and maintained in DMEM/F-12 medium supplemented with insulin (25 μg/ml), glucose (6 mg/ml), transferrin (100 μg/ml), progesterone (20 ng/ml), putrescine (60 μg/ml), and selenium (30 ng/ml). Cultured neurons were subjected to treatment after 6 days. Primary hippocampal neurons were cultured from E18 rat hippocampus. The cells were plated on poly-D-lysine-coated plates and cultured in neurobasal medium supplemented with B27 for 24 days before the treatment. Rat pheochromocytoma (PC12) cells were cultured as described previously (83) in RPMI 1640 medium supplemented with 10% heat-inactivated horse serum and 5% heat-inactivated fetal bovine serum. Neuronal differentiation was induced by NGF (50 ng/ml) in medium containing 1% horse serum for 6 days before the treatment.

Preparation of Amyloid—HPLC-purified Aβ(1–42) was purchased from American Peptide (Sunnyvale, CA), and oligomeric Aβ(1–42) was prepared. Lyophilized Aβ(1–42) was reconstituted in HFIP to 1 mM; HFIP was then removed by evaporation in a SpeedVac, and it was then resuspended to a concentration of 5 mM in anhydrous DMSO. This stock was then stored in −80 °C. The stock was further diluted with PBS to a final concentration of 400 μM, and SDS was added to a final concentration of 0.2%. The resulting solution was incubated at 37 °C for 18–24 h. The preparation was finally diluted with PBS to a final concentration of 100 μM and incubated at 37 °C for 18–24 h before use.

Oligomeric Aβ Treatment to Cells—Oligomeric Aβ(1–42) was added to the medium containing cells for the specific time points. The concentrations used were 1.5 μM for primary cultured rat cortical neurons and hippocampal neurons and 5 μM for neuronally differentiated PC12 cells (38, 44).

PCR—Total RNA for each sample is isolated from cultured cortical neurons by using TRI Reagent (Sigma). The primers used for PCR amplification of rat *Trib3* were 5′-GTTGCGTCGATTTGTCTTCA-3′ and 5′-CGGGAGCTGAGTATCTCTGG-3′. The primers for *GAPDH* were 5′-TCAACAGCAACTCCCACTCTT-3′ and 5′-ACCCTGTTGCTGTAGCCGTAT-3′. Equal amounts of cDNA template were used for each PCR analysis of *Trib3* or *GAPDH*. Primers were used at 0.2 μM concentration. For semi-quantitative PCR, products were analyzed on a 1.5% agarose gel and visualized by staining with ethidium bromide. Quantitative PCR were performed using One Step SYBR *Ex Taq* qRT-Takara by using Applied Biosystems 7500 Fast Real Time PCR System following the manufacturer's specifications.

Western Blotting Analysis—Cortical neurons and neuronally differentiated PC12 cells were lysed, and proteins were analyzed by Western blotting as described previously (65). For each condition 50 μg of protein were resolved in 4–12% SDS-PAGE and then transferred to PVDF membrane (Hybond: GE Healthcare, Buckinghamshire, UK). HRP-conjugated secondary antibodies against the primary antibodies were used. Detection was carried out by Amersham Biosciences ECL Western blotting detection reagent, according to the manufacturer's protocol. Imaging of all Western blottings was performed using an UVP BioImager 600 system equipped with Vision Works Life Science software, version 6.80 (UVP, Cambridge, UK).

Immunocytochemical Staining—Cortical neurons and neuronally differentiated PC12 cells were fixed with 4% paraformaldehyde for 10 min. Cells were then washed three times with PBS for 5 min each and then blocked in 3% goat serum in PBS containing 0.3% Triton X-100 for 2 h at room temperature. The cells were immunolabeled with primary antibody in a blocking solution overnight at 4 °C. The next day, cells were washed in PBS, followed by incubation with the appropriate secondary antibody for 2 h at room temperature. Nuclei were stained with Hoechst. High resolution images were taken using a Leica TCS SP8 microscope (Germany). The intensities of staining for control or treated cells were quantified separately by ImageJ software. The corrected total cell fluorescence (CTCF) was determined by considering the integrated density of staining, area of the cell, and the background fluorescence for the different experimental conditions. CTCF = integrated density − (area of selected cell × mean fluorescence of background readings).

TUNEL Assay—Detection of TUNEL-positive cells using *in situ* cell death detection kit was performed following the manufacturer's protocol.

Mitochondrial Staining—Cellular mitochondria were detected using MitoTracker red dye following the manufacturer's protocol.

Immunoprecipitation—Primary cultured cortical neurons were either treated with 1.5 μM Aβ for 8 h or left as untreated control, and interactions of Trib3 with Akt were detected by co-immunoprecipitation assays. The cells were washed with PBS and lysed in lysis buffer. For immunoprecipitation, agarose-conjugated anti-Trib3 antibody was prepared by incubating 3 μg of anti-Trib3 antibody with 20 μl of protein A-agarose beads for 2 h at 4 °C under shaking conditions. The agarose-conjugated Trib3 antibodies were then pelleted down and incubated with treated and untreated cell lysates containing equal amounts of protein overnight. This was kept at 4 °C under shaking condition. The antigen-antibody complexes were isolated and dissociated by boiling in sample buffer for 4 min. The agarose beads were pelleted down, and the supernatant was subjected to Western blotting analysis, as described previously using anti-Akt as the primary antibody.

Chromatin Immunoprecipitation (ChIP)—ChIP assays were done by using ChIP assay kit from Millipore (Billerica, MA) following manufacturer's protocol with few exceptions. $5–8 \times 10^6$ cortical neurons were used after treatment with or without Aβ. Rabbit polyclonal anti-FoxO1 antibody was used to immunoprecipitate the protein-DNA complexes. The primers used for PCR amplification of the rat *Trib3* promoter were forward 5′-GTGCTGGGACTCCGAGATAG-3′ and reverse 5′-CAACCTTCTTGCCAGACCTC-3′ (23). PCR products were analyzed on a 1.5% agarose gel and visualized by staining with ethidium bromide.

Transfection—DNA was isolated using plasmid maxi kit from Qiagen. For survival assay, cortical, hippocampal neurons, and PC12 cells were transfected with 0.5 μg of either pSIREN-Trib3-shRNA-zsgreen (shTrib3) or pSIREN-Rand-shRNA-zsgreen (shRand), pWPI plasmid containing Trib3 overexpression vector, and the corresponding control plasmid. Transfections were done in 500 μl of serum-free medium per well of a 24-well plate using Lipofectamine 2000. Five hours later, Lipofectamine-containing medium was replaced by fresh medium. Transfection was performed on the 3rd day of culture for primary cortical neurons and on the 19th day of culture for primary hippocampal neurons. Differentiated neuronal PC12 cells were transfected on the 3rd day of differentiation. For endogenous Trib3 down-regulation, naive PC12 cells were transfected with either 1 μg of shTrib3 or shRand. Transfections were done in 1 ml of serum-free medium per well of a 12-well plate using Lipofectamine 2000. 24 h post-transfection, cells were differentiated in presence of NGF. After 5 days of priming, cells were treated with either Aβ (5 μM) or left as untreated control.

Sholl Analysis—Sholl analysis was performed to analyze the neuritic branching and complexities of neuronal processes using ImageJ software as described previously (39) with a few modifications delineated below. Primary hippocampal neurons (19DIV) were transfected with shFoxO or shRand as described previously. A fluorescence microscope was used to image the transfected neurons. Low magnification pictures of single neurons were taken at 0 and 48 h of Aβ(1–42) treatment. Sholl analysis was performed on these images using ImageJ software (Sholl analysis plugin). A number of concentric circles were drawn projecting from the cell body with gradually increasing radii of 40 mm in length. Two-dimensional analyses were performed to count the number of branches that intersect the successive concentric circle. Data are represented as mean ± S.E. of four neurons from three independent experiments.

Survival Assay—Primary cortical neurons (3DIV) and primary hippocampal neurons (22DIV) were transfected with shRand or shTrib3 as mentioned above. 48 h post-transfection, the neurons were exposed to Aβ(1–42), and the number of transfected neurons (green) was counted (0 h) under the microscope. The number of surviving transfected neurons was also counted after 24, 48, and 72 h of treatment as described previously (49). Control and Aβ-treated transfected neurons were imaged under a fluorescence microscope (Leica, Wetzlar, Germany). Data are represented as mean ± S.E. of three independent experiments, which were performed in triplicate.

Oligomeric Aβ Infusion in Animals —Five Male Sprague-Dawley rats (300–380 g) were infused with oligomeric Aβ as described previously, and five male rats were infused with PBS. Briefly, rats were anesthetized by injecting a mixture of xylazine/ketamine and placed on a stereotaxic frame. A volume of 5 μl of 100 μM Aβ in PBS was infused in the right cerebral cortex at stereotaxic coordinates from bregma: anterior-posterior, 4.1 mm, λ, 2.5 mm, dorsal-ventral, 1.3 mm, according to the rat brain atlas and a previous report (84). Equal volume of PBS was injected in control animals. Animals were sacrificed 21 days post-injection. The brains were dissected out following cardiac perfusion and fixed in 4% paraformaldehyde for 24 h. The brains were further incubated in a 30% sucrose solution for 24 h, and then cryo-sectioning was performed by using a cryotome (Thermo Fisher Scientific, West Palm Beach, FL).

Immunohistochemistry of Brain Slices—Cryosections measuring 20 μm of the brains from Aβ-infused or PBS-infused rats and wild-type or transgenic mice were immunostained as described previously. Briefly, sections were blocked with 5% goat serum in PBS containing 0.3% Triton X-100 for 1 h at room temperature; sections were incubated in primary antibody in a blocking solution overnight at 4 °C. The following day, the sections were washed three times with PBS and then incubated with a fluorescence-tagged secondary antibody for 2 h at room temperature. Hoechst staining for the nucleus was performed. The sections were mounted and observed under fluorescence microscope.

Statistics—All experimental results are reported as mean ± S.E. Student's *t* test was performed as unpaired two-tailed sets of arrays to evaluate the significance of difference between the means and are presented as *p* values.

Author Contributions—S. C. B. and S. S. conceived the idea, designed the experiments, analyzed the data, and wrote the manuscript. S. S. performed all experiments.

Acknowledgments—We thank Dr. A. B. Patel (Council of Scientific and Industrial Research-CCMB, Hyderabad, India) for providing tissues of transgenic animals of Alzheimer's model and Priyankar Sanphui for help processing the transgenic brains. We thank Dr. Lloyd Greene and Dr. Neela Zareen (Columbia University) for providing Trib3 constructs. We also thank Dr. P. K. Sarkar for critical reading of this manuscript and helpful discussions.

References

1. Serrano-Pozo, A., Frosch, M. P., Masliah, E., and Hyman, B. T. (2011) Neuropathological alterations in Alzheimer disease. *Cold Spring Harb. Perspect. Med.* **1,** a006189
2. Finder, V. H., and Glockshuber, R. (2007) Amyloid-β aggregation. *Neurodegener. Dis.* **4,** 13–27
3. Tanzi, R. E., and Bertram, L. (2005) Twenty years of the Alzheimer's disease amyloid hypothesis: a genetic perspective. *Cell* **120,** 545–555
4. Selkoe, D. J. (2001) Alzheimer's disease: genes, proteins, and therapy. *Physiol. Rev.* **81,** 741–766
5. LaFerla, F. M., Green, K. N., and Oddo, S. (2007) Intracellular amyloid-β in Alzheimer's disease. *Nat. Rev. Neurosci.* **8,** 499–509
6. Salminen, A., Kauppinen, A., Suuronen, T., Kaarniranta, K., and Ojala, J. (2009) ER stress in Alzheimer's disease: a novel neuronal trigger for inflammation and Alzheimer's pathology. *J. Neuroinflammation* **6,** 41
7. Salazar, M., Carracedo, A., Salanueva, I. J., Hernández-Tiedra, S., Lorente, M., Egia, A., Vázquez, P., Blázquez, C., Torres, S., García, S., Nowak, J., Fimia, G. M., Piacentini, M., Cecconi, F., Pandolfi, P. P., *et al.* (2009) Cannabinoid action induces autophagy-mediated cell death through stimulation of ER stress in human glioma cells. *J. Clin. Invest.* **119,** 1359–1372
8. François, A., Rioux Bilan, A., Quellard, N., Fernandez, B., Janet, T., Chassaing, D., Paccalin, M., Terro, F., and Page, G. (2014) Longitudinal follow-up of autophagy and inflammation in brain of APPswePS1dE9 transgenic mice. *J. Neuroinflammation* **11,** 139
9. Nixon, R. A., Mathews, P. M., and Cataldo, A. M. (2001) The neuronal endosomal-lysosomal system in Alzheimer's disease. *J. Alzheimers Dis.* **3,** 97–107
10. Ling, D., Song, H. J., Garza, D., Neufeld, T. P., and Salvaterra, P. M. (2009) Aβ42-induced neurodegeneration via an age-dependent autophagic-lysosomal injury in *Drosophila*. *PLoS ONE* **4,** e4201
11. Hung, S. Y., Huang, W. P., Liou, H. C., and Fu, W. M. (2009) Autophagy protects neuron from Aβ-induced cytotoxicity. *Autophagy* **5,** 502–510
12. Jaeger, P. A., and Wyss-Coray, T. (2009) All-you-can-eat: autophagy in neurodegeneration and neuroprotection. *Mol. Neurodegener.* **4,** 16
13. Boland, B., Kumar, A., Lee, S., Platt, F. M., Wegiel, J., Yu, W. H., and Nixon, R. A. (2008) Autophagy induction and autophagosome clearance in neurons: relationship to autophagic pathology in Alzheimer's disease. *J. Neurosci.* **28,** 6926–6937
14. Salazar, M., Carracedo, A., Salanueva, I. J., Hernández-Tiedra, S., Egia, A., Lorente, M., Vázquez, P., Torres, S., Iovanna, J. L., Guzmán, M., Boya, P., and Velasco, G. (2009) TRB3 links ER stress to autophagy in cannabinoid anti-tumoral action. *Autophagy* **5,** 1048–1049
15. Vara, D., Salazar, M., Olea-Herrero, N., Guzmán, M., Velasco, G., and Díaz-Laviada, I. (2011) Anti-tumoral action of cannabinoids on hepatocellular carcinoma: role of AMPK-dependent activation of autophagy. *Cell Death Differ.* **18,** 1099–1111
16. Ord, D., and Ord, T. (2005) Characterization of human NIPK (TRB3, SKIP3) gene activation in stressful conditions. *Biochem. Biophys. Res. Commun.* **330,** 210–218
17. Hua, F., Mu, R., Liu, J., Xue, J., Wang, Z., Lin, H., Yang, H., Chen, X., and Hu, Z. (2011) TRB3 interacts with SMAD3 promoting tumor cell migration and invasion. *J. Cell Sci.* **124,** 3235–3246
18. Ord, D., Meerits, K., and Ord, T. (2007) TRB3 protects cells against the growth inhibitory and cytotoxic effect of ATF4. *Exp. Cell Res.* **313,** 3556–3567
19. Takahashi, Y., Ohoka, N., Hayashi, H., and Sato, R. (2008) TRB3 suppresses adipocyte differentiation by negatively regulating PPARγ transcriptional activity. *J. Lipid Res.* **49,** 880–892
20. Sakai, S., Ohoka, N., Onozaki, K., Kitagawa, M., Nakanishi, M., and Hayashi, H. (2010) Dual mode of regulation of cell division cycle 25 A protein by TRB3. *Biol. Pharm. Bull.* **33,** 1112–1116
21. Ohoka, N., Yoshii, S., Hattori, T., Onozaki, K., and Hayashi, H. (2005) TRB3, a novel ER stress-inducible gene, is induced via ATF4-CHOP pathway and is involved in cell death. *EMBO J.* **24,** 1243–1255
22. Wennemers, M., Bussink, J., Scheijen, B., Nagtegaal, I. D., van Laarhoven, H. W., Raleigh, J. A., Varia, M. A., Heuvel, J. J., Rouschop, K. M., Sweep, F. C., and Span, P. N. (2011) Tribbles homolog 3 denotes a poor prognosis in breast cancer and is involved in hypoxia response. *Breast Cancer Res.* **13,** R82
23. Zareen, N., Biswas, S. C., and Greene, L. A. (2013) A feed-forward loop involving Trib3, Akt and FoxO mediates death of NGF-deprived neurons. *Cell Death Differ.* **20,** 1719–1730
24. Corcoran, C. A., Luo, X., He, Q., Jiang, C., Huang, Y., and Sheikh, M. S. (2005) Genotoxic and endoplasmic reticulum stresses differentially regulate TRB3 expression. *Cancer Biol. Ther.* **4,** 1063–1067
25. Wu, M., Xu, L. G., Zhai, Z., and Shu, H. B. (2003) SINK is a p65-interacting negative regulator of NF-κB-dependent transcription. *J. Biol. Chem.* **278,** 27072–27079
26. Zhang, J., Wen, H. J., Guo, Z. M., Zeng, M. S., Li, M. Z., Jiang, Y. E., He, X. G., and Sun, C. Z. (2011) TRB3 overexpression due to endoplasmic reticulum stress inhibits AKT kinase activation of tongue squamous cell carcinoma. *Oral Oncol.* **47,** 934–939
27. Aimé, P., Sun, X., Zareen, N., Rao, A., Berman, Z., Volpicelli-Daley, L., Bernd, P., Crary, J. F., Levy, O. A., and Greene, L. A. (2015) Trib3 is elevated in Parkinson's disease and mediates death in Parkinson's disease models. *J. Neurosci.* **35,** 10731–10749
28. Zou, C. G., Cao, X. Z., Zhao, Y. S., Gao, S. Y., Li, S. D., Liu, X. Y., Zhang, Y., and Zhang, K. Q. (2009) The molecular mechanism of endoplasmic reticulum stress-induced apoptosis in PC-12 neuronal cells: the protective effect of insulin-like growth factor I. *Endocrinology* **150,** 277–285
29. Boudeau, J., Miranda-Saavedra, D., Barton, G. J., and Alessi, D. R. (2006) Emerging roles of pseudokinases. *Trends Cell Biol.* **16,** 443–452
30. Kiss-Toth, E., Bagstaff, S. M., Sung, H. Y., Jozsa, V., Dempsey, C., Caunt, J. C., Oxley, K. M., Wyllie, D. H., Polgar, T., Harte, M., O'Neill, L. A., Qwarnstrom, E. E., and Dower, S. K. (2004) Human tribbles, a protein family controlling mitogen-activated protein kinase cascades. *J. Biol. Chem.* **279,** 42703–42708
31. Hegedus, Z., Czibula, A., and Kiss-Toth, E. (2006) Tribbles: novel regulators of cell function; evolutionary aspects. *Cell. Mol. Life Sci.* **63,** 1632–1641
32. Liew, C. W., Bochenski, J., Kawamori, D., Hu, J., Leech, C. A., Wanic, K., Malecki, M., Warram, J. H., Qi, L., Krolewski, A. S., and Kulkarni, R. N. (2010) The pseudokinase tribbles homolog 3 interacts with ATF4 to negatively regulate insulin exocytosis in human and mouse beta cells. *J. Clin. Invest.* **120,** 2876–2888
33. Qi, L., Heredia, J. E., Altarejos, J. Y., Screaton, R., Goebel, N., Niessen, S., Macleod, I. X., Liew, C. W., Kulkarni, R. N., Bain, J., Newgard, C., Nelson, M., Evans, R. M., Yates, J., and Montminy, M. (2006) TRB3 links the E3 ubiquitin ligase COP1 to lipid metabolism. *Science* **312,** 1763–1766
34. Huang, Y., and Mucke, L. (2012) Alzheimer mechanisms and therapeutic strategies. *Cell* **148,** 1204–1222
35. Musiek, E. S., and Holtzman, D. M. (2015) Three dimensions of the amyloid hypothesis: time, space and 'wingmen'. *Nat. Neurosci.* **18,** 800–806
36. Gilbert, B. J. (2013) The role of amyloid β in the pathogenesis of Alzheimer's disease. *J. Clin. Pathol.* **66,** 362–366
37. Lesné, S. E., Sherman, M. A., Grant, M., Kuskowski, M., Schneider, J. A., Bennett, D. A., and Ashe, K. H. (2013) Brain amyloid-β oligomers in ageing and Alzheimer's disease. *Brain* **136,** 1383–1398
38. Sanphui, P., and Biswas, S. C. (2013) FoxO3a is activated and executes neuron death via Bim in response to β-amyloid. *Cell Death Dis.* **4,** e625

39. Cuesto, G., Enriquez-Barreto, L., Caramés, C., Cantarero, M., Gasull, X., Sandi, C., Ferrús, A., Acebes, Á., and Morales, M. (2011) Phosphoinositide-3-kinase activation controls synaptogenesis and spinogenesis in hippocampal neurons. *J. Neurosci.* **31,** 2721–2733
40. He, L., Simmen, F. A., Mehendale, H. M., Ronis, M. J., and Badger, T. M. (2006) Chronic ethanol intake impairs insulin signaling in rats by disrupting Akt association with the cell membrane. Role of TRB3 in inhibition of Akt/protein kinase B activation. *J. Biol. Chem.* **281,** 11126–11134
41. Cravero, J. D., Carlson, C. S., Im, H. J., Yammani, R. R., Long, D., and Loeser, R. F. (2009) Increased expression of the Akt/PKB inhibitor TRB3 in osteoarthritic chondrocytes inhibits insulin-like growth factor 1-mediated cell survival and proteoglycan synthesis. *Arthritis Rheum.* **60,** 492–500
42. Du, K., Herzig, S., Kulkarni, R. N., and Montminy, M. (2003) TRB3: a tribbles homolog that inhibits Akt/PKB activation by insulin in liver. *Science* **300,** 1574–1577
43. Lee, H. K., Kumar, P., Fu, Q., Rosen, K. M., and Querfurth, H. W. (2009) The insulin/Akt signaling pathway is targeted by intracellular β-amyloid. *Mol. Biol. Cell* **20,** 1533–1544
44. Akhter, R., Sanphui, P., and Biswas, S. C. (2014) The essential role of p53-up-regulated modulator of apoptosis (Puma) and its regulation by FoxO3a transcription factor in β-amyloid-induced neuron death. *J. Biol. Chem.* **289,** 10812–10822
45. Furuyama, T., Nakazawa, T., Nakano, I., and Mori, N. (2000) Identification of the differential distribution patterns of mRNAs and consensus binding sequences for mouse DAF-16 homologues. *Biochem. J.* **349,** 629–634
46. Sandelin, A., Alkema, W., Engström, P., Wasserman, W. W., and Lenhard, B. (2004) JASPAR: an open-access database for eukaryotic transcription factor binding profiles. *Nucleic Acids Res.* **32,** D91–D94
47. Farré, D., Roset, R., Huerta, M., Adsuara, J. E., Roselló, L., Albà, M. M., and Messeguer, X. (2003) Identification of patterns in biological sequences at the ALGGEN server: PROMO and MALGEN. *Nucleic Acids Res.* **31,** 3651–3653
48. Xuan, Z., and Zhang, M. Q. (2005) From worm to human: bioinformatics approaches to identify FOXO target genes. *Mech. Ageing Dev.* **126,** 209–215
49. Biswas, S. C., Shi, Y., Sproul, A., and Greene, L. A. (2007) Pro-apoptotic Bim induction in response to nerve growth factor deprivation requires simultaneous activation of three different death signaling pathways. *J. Biol. Chem.* **282,** 29368–29374
50. Gilley, J., Coffer, P. J., and Ham, J. (2003) FOXO transcription factors directly activate bim gene expression and promote apoptosis in sympathetic neurons. *J. Cell Biol.* **162,** 613–622
51. Pajak, B., Songin, M., Strosznajder, J. B., Orzechowski, A., and Gajkowska, B. (2009) Ultrastructural evidence of amyloid β-induced autophagy in PC12 cells. *Folia Neuropathol.* **47,** 252–258
52. Kim, J., Kundu, M., Viollet, B., and Guan, K. L. (2011) AMPK and mTOR regulate autophagy through direct phosphorylation of Ulk1. *Nat. Cell Biol.* **13,** 132–141
53. Shen, H. M., and Codogno, P. (2011) Autophagic cell death: Loch Ness monster or endangered species? *Autophagy* **7,** 457–465
54. Gottlieb, R. A., and Mentzer, R. M. (2010) Autophagy during cardiac stress: joys and frustrations of autophagy. *Annu. Rev. Physiol.* **72,** 45–59
55. Kuusisto, E., Salminen, A., and Alafuzoff, I. (2002) Early accumulation of p62 in neurofibrillary tangles in Alzheimer's disease: possible role in tangle formation. *Neuropathol Appl. Neurobiol.* **28,** 228–237
56. Bjørkøy, G., Lamark, T., Pankiv, S., Øvervatn, A., Brech, A., and Johansen, T. (2009) Monitoring autophagic degradation of p62/SQSTM1. *Methods Enzymol.* **452,** 181–197
57. Cardinale, A., Racaniello, M., Saladini, S., De Chiara, G., Mollinari, C., de Stefano, M. C., Pocchiari, M., Garaci, E., and Merlo, D. (2012) Sublethal doses of β-amyloid peptide abrogate DNA-dependent protein kinase activity. *J. Biol. Chem.* **287,** 2618–2631
58. Onoue, S., Endo, K., Ohshima, K., Yajima, T., and Kashimoto, K. (2002) The neuropeptide PACAP attenuates β-amyloid (1–42)-induced toxicity in PC12 cells. *Peptides* **23,** 1471–1478
59. Song, M. S., Baker, G. B., Todd, K. G., and Kar, S. (2011) Inhibition of β-amyloid1–42 internalization attenuates neuronal death by stabilizing the endosomal-lysosomal system in rat cortical cultured neurons. *Neuroscience* **178,** 181–188
60. Zheng, L., Cedazo-Minguez, A., Hallbeck, M., Jerhammar, F., Marcusson, J., and Terman, A. (2012) Intracellular distribution of amyloid β peptide and its relationship to the lysosomal system. *Translational Neurodegeneration* **1,** 19
61. Hegde, M. L., Anitha, S., Latha, K. S., Mustak, M. S., Stein, R., Ravid, R., and Rao, K. S. (2004) First evidence for helical transitions in supercoiled DNA by amyloid β peptide (1–42) and aluminum: a new insight in understanding Alzheimer's disease. *J. Mol. Neurosci.* **22,** 19–31
62. Ohyagi, Y., Asahara, H., Chui, D. H., Tsuruta, Y., Sakae, N., Miyoshi, K., Yamada, T., Kikuchi, H., Taniwaki, T., Murai, H., Ikezoe, K., Furuya, H., Kawarabayashi, T., Shoji, M., Checler, F., *et al.* (2005) Intracellular Aβ42 activates p53 promoter: a pathway to neurodegeneration in Alzheimer's disease. *FASEB J.* **19,** 255–257
63. Biswas, S. C., Liu, D. X., and Greene, L. A. (2005) Bim is a direct target of a neuronal E2F-dependent apoptotic pathway. *J. Neurosci.* **25,** 8349–8358
64. Biswas, S. C., Shi, Y., Vonsattel, J. P., Leung, C. L., Troy, C. M., and Greene, L. A. (2007) Bim is elevated in Alzheimer's disease neurons and is required for β-amyloid-induced neuronal apoptosis. *J. Neurosci.* **27,** 893–900
65. Biswas, S. C., and Greene, L. A. (2002) Nerve growth factor (NGF) down-regulates the Bcl-2 homology 3 (BH3) domain-only protein Bim and suppresses its proapoptotic activity by phosphorylation. *J. Biol. Chem.* **277,** 49511–49516
66. Wolfe, D. M., Lee, J. H., Kumar, A., Lee, S., Orenstein, S. J., and Nixon, R. A. (2013) Autophagy failure in Alzheimer's disease and the role of defective lysosomal acidification. *Eur. J. Neurosci.* **37,** 1949–1961
67. Liang, J. H., and Jia, J. P. (2014) Dysfunctional autophagy in Alzheimer's disease: pathogenic roles and therapeutic implications. *Neurosci. Bull.* **30,** 308–316
68. Son, J. H., Shim, J. H., Kim, K. H., Ha, J. Y., and Han, J. Y. (2012) Neuronal autophagy and neurodegenerative diseases. *Exp. Mol. Med.* **44,** 89–98
69. Moreira, P. I., Santos, R. X., Zhu, X., Lee, H. G., Smith, M. A., Casadesus, G., and Perry, G. (2010) Autophagy in Alzheimer's disease. *Expert Rev. Neurother.* **10,** 1209–1218
70. Jung, C. H., Ro, S. H., Cao, J., Otto, N. M., and Kim, D. H. (2010) mTOR regulation of autophagy. *FEBS Lett.* **584,** 1287–1295
71. Chen, T. J., Wang, D. C., and Chen, S. S. (2009) Amyloid-β interrupts the PI3K-Akt-mTOR signaling pathway that could be involved in brain-derived neurotrophic factor-induced Arc expression in rat cortical neurons. *J. Neurosci. Res.* **87,** 2297–2307
72. Huang, S., Okamoto, K., Yu, C., and Sinicrope, F. A. (2013) p62/sequestosome-1 up-regulation promotes ABT-263-induced caspase-8 aggregation/activation on the autophagosome. *J. Biol. Chem.* **288,** 33654–33666
73. Liu, Y., Shoji-Kawata, S., Sumpter, R. M., Jr, Wei, Y., Ginet, V., Zhang, L., Posner, B., Tran, K. A., Green, D. R., Xavier, R. J., Shaw, S. Y., Clarke, P. G., Puyal, J., and Levine, B. (2013) Autosis is a Na^+,K^+-ATPase-regulated form of cell death triggered by autophagy-inducing peptides, starvation, and hypoxia-ischemia. *Proc. Natl. Acad. Sci. U.S.A.* **110,** 20364–20371
74. Liu, Y., and Levine, B. (2015) Autosis and autophagic cell death: the dark side of autophagy. *Cell Death Differ.* **22,** 367–376
75. Ni, H. M., Du, K., You, M., and Ding, W. X. (2013) Critical role of FoxO3a in alcohol-induced autophagy and hepatotoxicity. *Am. J. Pathol.* **183,** 1815–1825
76. Sengupta, A., Molkentin, J. D., and Yutzey, K. E. (2009) FoxO transcription factors promote autophagy in cardiomyocytes. *J. Biol. Chem.* **284,** 28319–28331
77. Zhao, Y., Yang, J., Liao, W., Liu, X., Zhang, H., Wang, S., Wang, D., Feng, J., Yu, L., and Zhu, W. G. (2010) Cytosolic FoxO1 is essential for the induction of autophagy and tumour suppressor activity. *Nat. Cell Biol.* **12,** 665–675
78. Mammucari, C., Milan, G., Romanello, V., Masiero, E., Rudolf, R., Del Piccolo, P., Burden, S. J., Di Lisi, R., Sandri, C., Zhao, J., Goldberg, A. L.,

Schiaffino, S., and Sandri, M. (2007) FoxO3 controls autophagy in skeletal muscle *in vivo*. *Cell Metab.* **6,** 458–471
79. Xue, L., Fletcher, G. C., and Tolkovsky, A. M. (1999) Autophagy is activated by apoptotic signalling in sympathetic neurons: an alternative mechanism of death execution. *Mol. Cell. Neurosci.* **14,** 180–198
80. Ghavami, S., Shojaei, S., Yeganeh, B., Ande, S. R., Jangamreddy, J. R., Mehrpour, M., Christoffersson, J., Chaabane, W., Moghadam, A. R., Kashani, H. H., Hashemi, M., Owji, A. A., and Łos, M. J. (2014) Autophagy and apoptosis dysfunction in neurodegenerative disorders. *Prog. Neurobiol.* **112,** 24–49
81. Yang, D. S., Kumar, A., Stavrides, P., Peterson, J., Peterhoff, C. M., Pawlik, M., Levy, E., Cataldo, A. M., and Nixon, R. A. (2008) Neuronal apoptosis and autophagy cross talk in aging PS/APP mice, a model of Alzheimer's disease. *Am. J. Pathol.* **173,** 665–681
82. Troy, C. M., Rabacchi, S. A., Friedman, W. J., Frappier, T. F., Brown, K., and Shelanski, M. L. (2000) Caspase-2 mediates neuronal cell death induced by β-amyloid. *J. Neurosci.* **20,** 1386–1392
83. Greene, L. A., and Tischler, A. S. (1976) Establishment of a noradrenergic clonal line of rat adrenal pheochromocytoma cells which respond to nerve growth factor. *Proc. Natl. Acad. Sci. U.S.A.* **73,** 2424–2428
84. Frautschy, S. A., Baird, A., and Cole, G. M. (1991) Effects of injected Alzheimer β-amyloid cores in rat brain. *Proc. Natl. Acad. Sci. U.S.A.* **88,** 8362–8366